Radiative mass corrections at the two-loop order

July 14, 2017

Contents

1 Introduction

In this document we present a detailed calculation of radiative corrections up to two-loop order in the perturbative couplings for two quantum field theories. For the purposes of a clear and explanatory presentation we work through a scalar field theory example using all the tools available. This is followed by a more complicated calculation of the two-loop mass corrections in a triplet extended electroweak model.

The physical mass of a particle observed in experiments is not the $\overline{\text{MS}}$ mass appearing in a renormalised Lagrangian. Instead it is given by the *pole mass*, which is defined as the pole of the two-point propagator after finite renormalisation effects are taken into account. The form of the propagator, and thus the pole mass, depends on the field in question. For a scalar field, $\phi(x)$, the two-point propagator is given by

$$\langle\Omega|T\phi(x)\phi(y)|\Omega\rangle = \frac{i}{p^2 - m^2 + i\epsilon} + \frac{i}{p^2 - m^2 + i\epsilon}\left[-i\Sigma^{(1)}(p)\right]\frac{i}{p^2 - m^2 + i\epsilon} + \ \ldots \quad (1)$$

where the first term is the free field propagator, the second term is all the diagrams with two external legs and one-loop between them and the dots represent terms with two-loops, three-loops and so on. So $\Sigma^{(1)}$ is the sum of the amplitudes of all one particle irreducible processes (1PI) $\phi \to \phi$ that contain one-loop between the incoming and outgoing propagators. In this case a 1PI process is a diagram with two external scalar legs, which can not be split into a sum of such diagrams. Once we have evaluated $\Sigma^{(1)}$ we must include an infinite series of these 1PI diagrams. If one loop precision is required then one can set $\Sigma^{(1)} = \Sigma$, otherwise it may be left to represent higher order loop processes. After taking this infinite series of 1PI diagrams we end up with the Fourier transform of the two-point

function

$$\begin{aligned}\int \mathrm{d}^4x\, \langle\Omega|T\phi(x)\phi(0)|\Omega\rangle\, e^{-p\cdot x} =& \frac{i}{p^2-m^2} + \frac{i}{p^2-m^2}\left[-i\Sigma(p)\right]\frac{i}{p^2-m^2} \\ &+ \frac{i}{p^2-m^2}\left[-i\Sigma(p)\right]\frac{i}{p^2-m^2}\left[-i\Sigma(p)\right]\frac{i}{p^2-m^2} + \ \ldots\end{aligned} \tag{2}$$

Since $\Sigma(p)$ clearly commutes with i we are able to express this sum as a geometric series (this case is true for other propagators with momentum dependent numerators, since $\Sigma(p)$ is a function of $\not{p}$ and numbers only)

$$\begin{aligned}\int \mathrm{d}^4x\, \langle\Omega|T\phi(x)\phi(y)|\Omega\rangle\, e^{-p\cdot x} &= \frac{i}{p^2-m^2}\left(1 + \left(\frac{\Sigma(p)}{p^2-m^2}\right) + \left(\frac{\Sigma(p)}{p^2-m^2}\right)^2 + \ \ldots\right) \\ &= \frac{i}{p^2-m^2-\Sigma(p)}\end{aligned} \tag{3}$$

so the pole of the propagator is given by $p^2 = m^2 + \Sigma(p)$. The pole mass of a scalar field is therefore defined as $m_{\text{pole}} = p$ such that $p = \sqrt{m^2 + \Sigma(p)}$, where $\Sigma(p)$ is known as the *self energy*.

The above procedure can be repeated for other types of fields. For a Dirac fermion the free-field part of the propagator (equivalent to the first term in (1)) is

$$S_F(p) = \frac{i}{\not{p} - m + i\epsilon}. \tag{4}$$

After working through the same steps as for the scalar field theory we arrive at a Dirac fermion pole mass $m_{\text{pole}} = p$ for $p = m + \Sigma(p)$.

Finally we will need the self energy of gauge-bosons. The self energy of gauge-bosons can be separated into a transverse and a longitudinal piece as

$$\Sigma^{\mu\nu}_{ZZ}(p^2) \ = \ \Sigma^{T}_{ZZ}(p^2)\left[g^{\mu\nu} - \frac{p^\mu p^\nu}{p^2}\right] \ + \ \Sigma^{L}_{ZZ}(p^2)\,\frac{p^\mu p^\nu}{p^2} \ . \tag{5}$$

The physical gauge-boson masses are the poles of the corresponding propagators, which involve only the transverse part of the gauge-boson self-energy,

$$M_V^2 \ = \ \hat{M}_V^2 \ - \ \mathcal{R}e\,\Sigma^T_{VV}(M_Z^2) \ , \tag{6}$$

where $\hat{M}_V$ and $\hat{M}_V$ denote the $\overline{\text{MS}}$ mass of the gauge boson $V \in \{W, Z, \gamma, ...\}$.

The self-energies and $\overline{\text{MS}}$ masses are evaluated at a particular renormalization scale, μ^2. When possible, we have omitted the explicit dependance of these quantities on μ^2 as it

only has relevance when we wish to numerically evaluate the self energies.

Determining the value of the self energy, $\Sigma(p)$, is the focus of this work. As $\Sigma(p)$ is a perturbative quantity, we have in general

$$\Sigma(p) = \frac{1}{16\pi^2}\Sigma^{(1)}(p) + \frac{1}{(16\pi^2)^2}\Sigma^{(2)}(p) + \ \ldots \tag{7}$$

where $\Sigma^{(1)}(p)$ is the sum of all 1PI diagrams involving one-loop, $\Sigma^{(2)}(p)$ is all 1PI diagrams involving two loops and so on. In a valid perturbation theory the magnitude of the corrections will decrease with order such that the geometric series is convergent. Typically one or two-loop corrections are considered sufficient when comparing to the precision of modern experimental measurements.

The main purpose of this document is to make clear how we employ the computational tools available to calculate the radiative corrections in a manner consistent with existing results in the literature. In particular, we compare with results for a scalar field theory from Martin 2006 [1] and for the electroweak model with Ibe, Matsumoto and Sato 2013 [2]. We will make use of FeynArts [3] for generating amplitudes, FeynCalc [4, 5] for reducing these to integrals, TARCER [6] to further reduce these integrals to basis integrals and TSIL [1] to numerically evaluate these integrals.

The final step of converting TARCER output into an interface with TSIL is non-trivial in that it requires organisation and sorting of massive amounts of symbolic expressions. The amplitude produced by TARCER is written in terms of divergent basis integrals which we must also seperate into a divergent and finite piece. For this purpose, and for organising the entire calculation, we make use of the Mass Builder program (see attached program manual) which generates Mathematica scripts to perform the symbolic calculations, right from the initial amplitude generation with FeynArts, through to generating a C++ interface to the TSIL libraries to perform the numerical evaluation of the amplitudes.

2 Scalar field theory

2.1 Introduction

The field theory we will deal with here is that with Lagrangian

$$\mathcal{L} = \frac{1}{2}(\partial_\mu s)^2 - \frac{1}{2}m^2 s^2 - \frac{g}{3!}s^3 - \frac{\lambda}{4!}s^4 \tag{8}$$

where m is the Lagrangian mass parameter of the field and we have two couplings, g and λ, for the cubic and quartic interactions respectively. We now need to redefine the field and couplings in terms of renormalised $\overline{\text{MS}}$ parameters,

$$s \to Z_s^{1/2} s, \quad m^2 \to \frac{1}{Z_s}(m^2 + \delta m^2), \quad g \to \frac{1}{Z_s^{3/2}}(g + \delta_g), \quad \lambda \to \frac{1}{Z_s^2}(\lambda + \delta\lambda) \tag{9}$$

such that the Lagrangian becomes

$$\mathcal{L} = \mathcal{L}_{free} + \mathcal{L}_{interaction} \tag{10}$$

where

$$\mathcal{L}_{free} = \frac{1}{2}(\partial_\mu s)^2 - \frac{1}{2}m^2 s^2 \tag{11}$$

$$\mathcal{L}_{interaction} = -\frac{g}{3!}s^3 - \frac{\lambda}{4!}s^4 + \frac{1}{2}(Z_s - 1)(\partial_\mu s)^2 - \frac{\delta m}{2}m^2 s^2 - \frac{\delta g}{3!}s^3 - \frac{\delta\lambda}{4!}s^4 \tag{12}$$

We can use the above interaction Lagrangian to determine the Feynman rules for each vertex interaction. For the two-point propagator we have the tree-level counter-term with interaction coupling $i(Z_s - 1)k^2 - i\delta m$. We will define $Z_s - 1 = \delta Z$. The cubic and quartic interactions are simply $-i\delta g$ and $-i\delta\lambda$ respectively, with no momentum dependant part. The FeynArts model file that we have created for this model and use in the following calcualtions is provided with Mass Builder.

2.2 One-loop self energy

In this section we present the corrections to the scalar propagator that are of one-loop order, including the tree-level counter-term. Although these are easily written down by hand we use Mass Builder to carry out the calculation and demonstrate consistency.

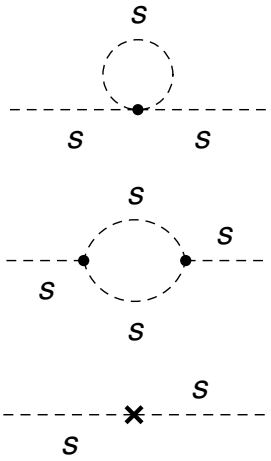

The "tadpole" diagram on the top left is the easiest to evaluate, the integral is

$$\Pi_1^{(1)} = \kappa\frac{\lambda}{2}\int \mathrm{d}^4k \frac{-i}{k^2 - m^2} = \kappa\frac{\lambda}{2}\mathbf{A}(m^2). \tag{13}$$

The result directly from TARCER is

$$\Pi_1^{(1)} = -i\kappa\frac{\lambda}{2}\mathbf{TAI}(m^2) \tag{14}$$

so after using the relationship $i\mathbf{TAI}(x) = \mathbf{A}(x)$ we see these are equivalent. The result here is a divergent integral, expressing it as a divergent plus finite piece we have

$$\Pi_1^{(1)} = \frac{1}{2}\kappa\lambda\left(A(m^2) + \epsilon A_\epsilon(m^2) - \frac{m^2}{\epsilon}\right). \tag{15}$$

For the second loop correction we can again immediately write down the integral

$$\Pi_2^{(1)} = -\kappa \frac{g^2}{2} \mathbf{B}(m^2, m^2). \tag{16}$$

and then use and $-i\mathbf{TBI} = \mathbf{B}$ to convert to TSIL notation

$$\Pi_2^{(1)} = -i\kappa \frac{g^2}{2} \mathbf{TBI}(m^2, m^2) \tag{17}$$

which is the output we obtain from TARCER. The finite plus divergent result is

$$\Pi_2^{(1)} = -\frac{1}{2}\kappa g^2 \left(B(m^2) + \epsilon B_\epsilon(m^2) + \frac{1}{\epsilon} \right). \tag{18}$$

The counter-term diagram is trivial to calculate by hand, yet again we will take the result from TARCER which is

$$\Pi_1^{(1c)} = \delta m - \delta Z p^2 \tag{19}$$

We now need to remove the divergent terms from (15) and (18) by determining the appropriate values for the counter-term couplings, δm and δZ. In this case this is a simple calculation, which can do by hand but is also available as a feature in Mass Builder to do automatically. The full one-loop self energy, including counter-terms, is

$$\Pi_1 = \frac{1}{2}\kappa\lambda \left(A(m^2) + \epsilon A_\epsilon(m^2) - \frac{m^2}{\epsilon} \right) - \frac{1}{2}\kappa g^2 \left(B(m^2) + \epsilon B_\epsilon(m^2) + \frac{1}{\epsilon} \right) + \delta m - \delta Z p^2 \tag{20}$$

where the divergent part is

$$\Pi_1^{1/\epsilon} = -\frac{1}{2\epsilon}\kappa \left(\lambda m^2 + g^2 \right) + \delta m - \delta Z p^2 \tag{21}$$

so we find

$$\delta m = \frac{\kappa}{2\epsilon} \left(g^2 + \lambda m^2 \right) + \mathcal{O}(\kappa^2) \tag{22}$$

$$\delta Z = \mathcal{O}(\kappa^2) \tag{23}$$

where we allow for high order terms which are required to cancel divergences from amplitudes above the one-loop order, which we will determine in the next section.

2.3 Two-loop self energy

There are 9 loop corrections and 5 counter-term corrections to the scalar propagator at the two-loop level. We present the results as output by TARCER and the required conversions to TSIL integrals on a diagram by diagram basis in this section. This enables a direct comparison between our results and that found in the TSIL manual [1]. For the first diagram we show the equivalence down to the level of finite integrals, for which the fully worked result from Mass Builder is most useful. For the rest we either omit this working or the equivalence is immediately evident, and leave the result as divergent integrals for brevity.

Diagram 1

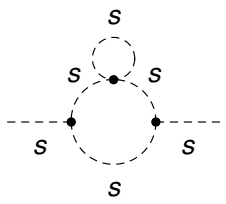

In integral form this diagram can be written down as

$$\Pi_1^{(2)} = -\kappa^2 \frac{\lambda g^2}{2} \mathbf{A}(x)\mathbf{B}(x',x) \tag{24}$$

using the definitions given in the appendix. However, we can't deal with derivatives of basis integrals with the computational tools we have as TARCER will always reduce to the most fundamental basis. So to make a proper check of the tools we must convert this to the most fundamental basis using the relationship

$$\mathbf{B}(x',y) = \Big[(3-d)(s-x+y)\mathbf{B}(x,y) + (2-d)\{\mathbf{A}(y) + (s-x-y)\mathbf{A}(x)/2x\}\Big]/\Delta_{sxy} \tag{25}$$

where

$$\Delta_{abc} \equiv a^2 + b^2 + c^2 - 2ab - 2ac - 2bc. \tag{26}$$

Now we will work through from the initial divergent basis integrals in (24) and obtain all finite contributions to the amplitude and compare this with the result from Mass Builder. First I deal with $\mathbf{B}_p(m^2, m^2)$. From (25) setting $x = y$ we have

$$\mathbf{B}(x',x) = \frac{2x(3-D)\mathbf{B}(x,x) + (2-D)\mathbf{A}}{2x(s-4x)} \tag{27}$$

Now we use the relationships $\mathbf{A}(\mathbf{x}) = -x/\epsilon + A(x)$ and $\mathbf{B}(x,y) = 1/\epsilon + B(x,y)$, along with setting $D = 4 - 2\epsilon$ to obtain

$$\begin{aligned}\Pi &= \frac{\left(-\frac{x}{\epsilon} + A(x)\right)\left[2x(2\epsilon-1)\left(\frac{1}{\epsilon} + B(x,x)\right) + (2\epsilon-2)\left(-\frac{x}{\epsilon} + A(x)\right)\right]}{2x(s-4x)} \\ &= \frac{1}{2x(s-4x)}\left(-2x^2 B(x,x) - 2A(x)B(x,x) - 2(A(x))^2\right)\end{aligned}$$

So setting $x = m^2$ and $s = p^2$ we have

$$\Pi = -\frac{g^2\lambda}{2(16\pi^2)^2}\frac{(2m^4B(m^2,m^2) + m^2A(m^2)B(m^2,m^2) + (A(m^2))^2)}{m^2(p^2-4m^2)} \tag{28}$$

Evaluating this diagram with Mass Builder we obtain the finite amplitude

$$\Pi = -\frac{g^2\lambda}{(16\pi^2)^2}\frac{(m^2A(m^2)B(m^2,m^2) + 2m^4B(m^2,m^2) + (A(m^2))^2)}{2m^2(4m^2-p^2)} \tag{29}$$

which agrees with the result computed by hand above.

Diagram 2 and 3

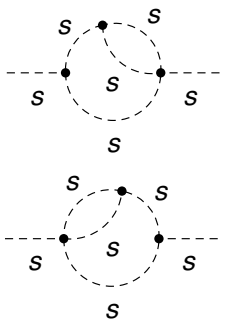

Diagrams 2 and 3 are identical and are given in TARCER to be

$$\Pi_2 = -\kappa^2\frac{g^2\lambda}{2}\mathbf{TVI}(m^2,m^2,m^2,m^2) \tag{30}$$

so combining these together and using the result $\mathbf{TVI} = -\mathbf{U}$ we obtain, the same result as we could get by simply looking at the topology of the diagram

$$\Pi_2 = \kappa^2 g^2\lambda\mathbf{U}(m^2,m^2,m^2,m^2). \tag{31}$$

Diagram 4

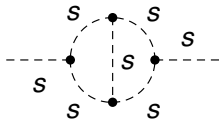

This diagram represents the “master" integral which has no divergences and is expressed, in the context of this amplitude, as

$$\Pi_4 = -\kappa^2\frac{g^4}{2}\mathbf{TFI}(m^2,m^2,m^2,m^2,m^2) \tag{32}$$

making the conversion to TSIL notation, $\mathbf{TFI} = \mathbf{M}$, we have

$$\begin{aligned}\Pi_4 &= -\kappa^2\frac{g^4}{2}\mathbf{M}(m^2,m^2,m^2,m^2,m^2)\\ &= -\kappa^2\frac{g^4}{2}M(m^2,m^2,m^2,m^2,m^2) + \mathcal{O}(\epsilon).\end{aligned} \tag{33}$$

Diagram 5

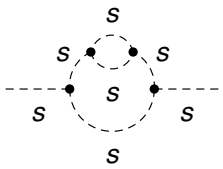

This diagram is given by TARCER to be, in terms of divergent integrals,

$$\begin{aligned}\Pi_5 = &-\kappa^2\frac{g^4}{12m^4}\left(\frac{3(3D-8)m^2(2m^2-p^2)}{p^2(4m^2-p^2)}\mathbf{TJI}(m^2,m^2,m^2)\right.\\ &+\frac{4m^2(m^2-p^2)(9m^2-p^2)}{p^2(4m^2-p^2)}\mathbf{TJI}_2(m^2,m^2,m^2)\\ &+\frac{3(D-2)m^2(2m^2-p^2)}{p^2(4m^2-p^2)}\mathbf{TKI}(m^2,m^2,m^2)\\ &+\frac{m^2(Dp^2+2(D-9)m^2)}{4m^2-p^2}\mathbf{TVI}(m^2,m^2,m^2,m^2)\\ &\left.+2(D-2)\mathbf{TAI}(m^2)\mathbf{TBI}(m^2,m^2)\right)\end{aligned} \tag{34}$$

converting to TSIL notation we obtain

$$\begin{aligned}\Pi_5 = &-\kappa^2\frac{g^4}{12m^4}\left(\frac{3(3D-8)m^2(2m^2-p^2)}{p^2(4m^2-p^2)}\mathbf{S}(m^2,m^2,m^2)\right.\\ &-\frac{4m^2(m^2-p^2)(9m^2-p^2)}{p^2(4m^2-p^2)}\mathbf{T}(m^2,m^2,m^2)\\ &+\frac{3(D-2)m^2(2m^2-p^2)}{p^2(4m^2-p^2)}\mathbf{I}(m^2,m^2,m^2)\\ &-\frac{m^2(Dp^2+2(D-9)m^2)}{4m^2-p^2}\mathbf{U}(m^2,m^2,m^2,m^2)\\ &\left.+2(D-2)\mathbf{A}(m^2)\mathbf{B}(m^2,m^2)\right)\end{aligned} \tag{35}$$

Diagram 6

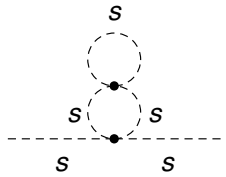

This diagram is given by TARCER to be

$$\Pi_6 = -\kappa^2\frac{\lambda^2(D-2)}{8}\frac{\left(\mathbf{TAI}(m^2)\right)^2}{m^2} \tag{36}$$

converting to TSIL notation and accounting for the negative sign we obtain

$$\Pi_6 = -\kappa^2\frac{\lambda^2(D-2)}{8}\frac{\left(\mathbf{A}(m^2)\right)^2}{m^2} \tag{37}$$

now we must set $D = 4 - 2\epsilon$ and account for finite contributions which come from the divergent parts of the basis integrals. The basis integrals can be expressed as a finite piece plus a divergent piece, so we have

$$\mathbf{TAI}(x) = \frac{ix}{\epsilon} + \texttt{TAI}(x) \tag{38}$$

where we have converted (1.28) of the TSIL manual [1] into the TARCER definition using $\mathbf{A} = ia\mathbf{TAI}$ and taking $a = 1$ for small ϵ (see the Mass Builder manual for the equivalent relationship for all basis integrals). So the amplitude becomes

$$\begin{aligned}\Pi_1 &= -\frac{\lambda^2(2-2\epsilon)}{8m^2}\left(\texttt{TAI}(m^2) + \frac{im^2}{\epsilon}\right)^2 \\ &= -\frac{\lambda^2}{4m^2}\texttt{TAI}(m^2)\left(\frac{\texttt{TAI}(m^2)}{m^2} - 2i\right)\end{aligned}$$

where we ignore any divergent terms (we will be careful to account for these properly later) and take the limit of $\epsilon \to 0$.

Finally we need to evaluate this in terms of TSIL integrals, which have a different normalization. The relationship is $\mathbf{A} = ia\mathbf{TAI}$ where $a = (4\pi\mu^2)^{2-D/2} \approx 1 + \frac{r\epsilon}{2}\log(4\pi\mu^2) + \mathcal{O}(\epsilon^2)$. Since we have already removed the divergent parts and are dealing with finite integrals, I take $\epsilon = 0$ and we simply have $\mathbf{A} = i\mathbf{TAI}$. Therefore we end up with

$$\Pi_1 = \kappa^2\frac{\lambda^2}{4}A(m^2)\left(\frac{A(m^2)}{m^2} + 2\right) \tag{39}$$

Diagram 7

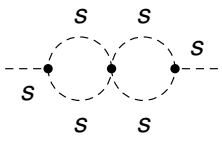

This diagram is given by TARCER to be

$$\Pi_7 = -\kappa^2\frac{g^2\lambda}{4}\left(\mathbf{TBI}(m^2, m^2)\right)^2 \tag{40}$$

using $-i\mathbf{TBI}(x, y) = \mathbf{B}(x, y)$ we obtain

$$\Pi_7 = \kappa^2\frac{g^2\lambda}{4}\left(\mathbf{B}(m^2, m^2)\right)^2 \tag{41}$$

Diagram 8

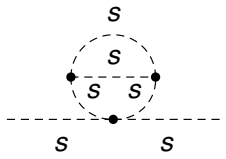

This diagram is given by TARCER to be

$$\Pi_8 = \kappa^2 \frac{g^2\lambda}{12m^2}(D-3)\mathbf{TKI}(m^2,m^2,m^2) \tag{42}$$

converting to TSIL notation and including a relative negative sign for the definition of the basis integral we obtain

$$\Pi_8 = -\kappa^2 \frac{g^2\lambda}{12m^2}(D-3)\mathbf{I}(m^2,m^2,m^2). \tag{43}$$

Diagram 9

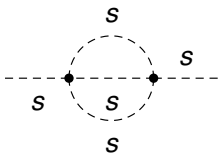

This diagram is given by TARCER to be

$$\Pi_9 = \kappa^2 \frac{\lambda^2 \mathbf{TJI}(m^2,m^2,m^2)}{6} \tag{44}$$

where $\mathbf{TJI} = \mathbf{TJI}\{1,1,1\}$ which is equivalent to the TSIL integral $S(x,y,z)$ for $a=1$, accounting for the negative sign we obtain

$$\Pi_9 = -\kappa^2 \frac{\lambda^2}{6}\mathbf{S}(m^2,m^2,m^2).$$

Counter-diagram 1

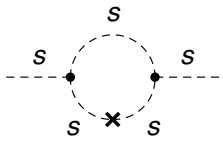

The first counter-term diagram involves a correction to the internal scalar propagator and has an amplitude given by TARCER to be

$$\Pi_1 = \kappa \frac{1}{\epsilon}\frac{id_1 g^2}{2m^2(4m^2-p^2)}\Big((D-2)\mathbf{TAI}(m^2) - 2(D-3)\mathbf{TBI}(m^2,m^2)\Big) \tag{45}$$

where we have also multiplied the computed result by $1/\epsilon$[1]. Converting to TSIL notation we find

$$\Pi_1 = \kappa \frac{d_1}{\epsilon}\frac{g^2}{2m^2(4m^2-p^2)}\Big((2-2\epsilon)\mathbf{A}(m^2) + 2(1-2\epsilon)\mathbf{B}(m^2,m^2)\Big) \tag{46}$$

[1] We could either include the $1/\epsilon$ in the definition of the counter-term coupling or insert it now, this keep the counter-term coupling as a finite quantity and enables us to identify what the finite terms are before determining the coupling.

from which we obtain the finite contribution

$$\Pi_1 = \kappa d_1 \frac{g^2}{2m^2(4m^2 - p^2)} \left(-2A(m^2) + 2A_\epsilon(m^2) - 4m^2 B(m^2, m^2) + 2Bm_\epsilon^2(m^2, m^2) \right). \tag{47}$$

Counter-diagram 2

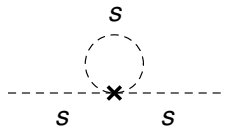

$$\Pi_2 = \frac{1}{\epsilon} \kappa i \frac{d_\lambda}{2} \mathbf{TAI}(m^2) \tag{48}$$

converting from TARCER to TSIL we obtain

$$\Pi_2 = -\frac{1}{\epsilon} \kappa \frac{d_\lambda}{2} \ \mathbf{A}(m^2) \tag{49}$$

which given the form of $\mathbf{A}(m^2)$ contains no finite contributions. However it is still required to set the value of d_λ and cancel the divergences from other diagrams.

Counter-diagram 3 and 5

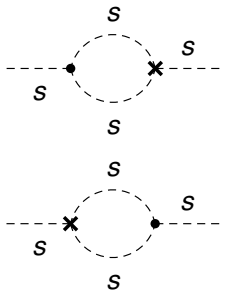

Counter-term diagrams 3 and 5 are identical and have a total amplitude of

$$\Pi_{3,5} = \kappa i \frac{g d_g}{\epsilon} \mathbf{TBI}(m^2, m^2) \tag{50}$$

converting to TSIL notation and inserting the counter-term coupling (each introduces a negative sign)

$$\Pi_{3,5} = \kappa^2 g \frac{c^g_{1,1}}{\epsilon} \mathbf{B}(m^2, m^2) \tag{51}$$

Counter-diagram 4

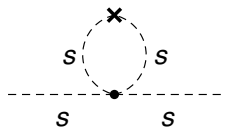

$$\Pi_4 = \frac{1}{\epsilon} \kappa \frac{i\lambda d_1 (D-2)}{4m^2} \mathbf{TAI}(m^2) \tag{52}$$

changing to TSIL notation we find

$$\Pi_4 = \frac{1}{\epsilon} \kappa \frac{\lambda d_1 (D-2)}{4m^2} \mathbf{A}(m^2) \tag{53}$$

2.4 The total finite mass correction

The final step is the most non-trivial and involves cancelling all divergences by a careful choice of counter-term couplings. We use Mathematica to solve a set of simultaneous equations for the counter-term couplings. There are five counter-terms to determine up to the order in ϵ we require, the first of these has already been calculated in the first section, leaving four to compute from the full amplitude.

If $\Pi = \sum_{i=1}^{2} \Pi_i^{(1)} + \sum_{i=1}^{9} \Pi_i^{(2)} + \Pi_1^{(1c)} + \sum_{i=1}^{5} \Pi_i^{(2c)}$ is the total self energy then we demand that Π has no terms of order one or higher in $1/\epsilon$. We take the coefficients of $1/\epsilon$, and $1/\epsilon^2$, and then subsequently take the coefficients of the $A(x)$ and $B(x,x)$ terms from each of these to form four seperate equations. These are sufficient to solve the system and obtain the following counter-terms

$$\delta\lambda = \kappa\frac{3\lambda^2}{2} \tag{54}$$

$$\delta g = \kappa\frac{3g\lambda}{2} \tag{55}$$

$$\delta Z = \frac{\kappa^2}{8}\left(7g^2\lambda + 4\lambda^2 m^2\right) \tag{56}$$

$$\delta m = \frac{\kappa}{2\epsilon}\left(g^2 + \lambda m^2\right) + \frac{\kappa^2}{24}\left(-15g^2\lambda + \lambda^2 p^2 - 6\lambda^2 m^2\right) \tag{57}$$

with these counter-term couplings all divergences are removed. In δm we used the result for the order κ part from the one-loop calculation in section 2.2. The resultant self energy is

$$\Pi^{(1)}(p^2) = \frac{1}{2}\lambda A(x) - \frac{1}{2}g^2 B(x,x) \tag{58}$$

$$\begin{aligned}\Pi^{(2)}(p^2) = &-\frac{1}{2}g^4 M(x,x,x,x,x) - \frac{1}{2}g^4 V(x,x,x,x) + \lambda g^2 U(x,x,x,x) \\ &-\frac{1}{6}\lambda^2 S(x,x,x) + \frac{1}{4}\lambda g^2 B(x,x)B(x,x) + \frac{1}{4}\lambda^2 A(x)\left[A(x)/x + 1\right] \\ &-\frac{1}{2}\lambda g^2 A(x)B(x',x) - \frac{1}{4}\lambda g^2 I(x',x,x)\ ,\end{aligned} \tag{59}$$

where $x = m^2$. This result contains only finite basis integrals and note that all coefficients of the $A_\epsilon(x)$ and $B_\epsilon(x,x)$ functions are zero in the total amplitude.

3 Massless QED

3.1 Introduction

Massless quantum electrodynamics (QED) is a minimal theory containing a gauge boson and lepton fields. I use the massless theory here as it admits analytic expressions for all

two-loop amplitudes which I can then compare with the numerical results.
The bare Lagrangian is

$$\mathcal{L} = -\frac{1}{4}F_{B\mu\nu}F_B^{\mu\nu} + \Sigma_f \bar{\psi}_{f,B}\left(i\partial_\mu - e_{f,B}A_{B\mu}\right)\psi_{f,B} \tag{60}$$

where $F_{B\mu\nu} = \partial_\mu A_{B\nu} - \partial_\nu A_{B\mu}$ and f is the flavour index. The renormalised Lagrangian is given by

$$\mathcal{L}_{\text{ren}} = -\frac{1}{4}F_{\mu\nu}F^{\mu\nu} + \Sigma_f \bar{\psi}_f\left(i\partial_\mu - e_f A_\mu\right)\psi_f \tag{61}$$

$$\mathcal{L}_{\text{ct}} = -\sum_f e_f \delta_{f,1}\psi_f A_\mu \gamma^\mu \psi_f + \sum_f \delta_{f,2} i\bar{\psi}_f \partial_\mu \gamma^\mu \psi_f - \frac{\delta_3}{4}F_{\mu\nu}F^{\mu\nu} \tag{62}$$

I will focus in this section on the self energy of the $f = e$ flavour state.

3.2 One-loop self energies

I present the one-loop self energies for the photon and the lepton state. The amplitudes and the analytic expressions for the integrated forms are taken from Sato [7] and are compared with the same amplitude as computed using Mass Builder .

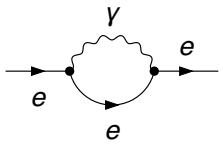

The one-loop amplitude for the fermion is given by the integral [7]

$$i\Sigma^{(1)} = -e^2\mu^{4-d}\int \frac{d^dk}{(2\pi)^d}\frac{\gamma^\mu \not{k}\gamma_\mu}{k^2(k-p)^2} \tag{63}$$

which is evaluated to be [7]

$$i\Sigma^{(1)} = \frac{e^2\not{p}}{16\pi^2}\left(\frac{1}{\epsilon}+1\right)\left(\frac{-p^2}{Q^2}\right)^{-\epsilon} + \mathcal{O}(\epsilon) \tag{64}$$

The finite part of this is compared with the output from Mass Builder and is found to be in agreement.

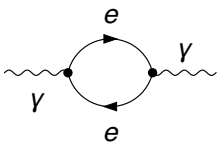

The one-loop amplitude for the photon is given by the integral [7]

$$i\Pi^{(1)}_{\mu\nu} = -e^2\mu^{4-d}\int \frac{d^dk}{(2\pi)^d}\frac{\mathrm{Tr}[\gamma^\mu \not{k}\gamma^\nu(\not{k}-\not{p})]}{k^2(k-p)^2} \tag{65}$$

which is evaluated to be [7]

$$i\Pi^{(1)} = \sum_f \frac{ie^2}{16\pi^2}\left(\frac{4}{3\epsilon}+\frac{20}{9}\right)\left(\frac{-p^2}{Q^2}\right)^{-\epsilon}(p^2 g_{\mu\nu}-p_\mu p_\nu)+\mathcal{O}(\epsilon) \tag{66}$$

The finite part of this is compared with the output from Mass Builder and is found to be in agreement.

3.3 Two-loop self energy

In this section I will present the two-loop self energy for the electron flavoured lepton. I will compare results from Sato [7], FeynHelpers [8], Grozin [9] with that computed using the Mass Builder package. To understand the differences I present the full UV divergent amplitudes, which are not usually output from Mass Builder but can be obtained by running the generated Mathematica scripts (which are made available via the −v flag at run time).

3.3.1 Required notation

The quantities we will need for the comparisons from various authors are given below. The TARCER basis integral TJI[D, SPD[p, p], {{1, 0}, {1, 0}, {1, 0}}] is given by [6]

$$\mathbf{J}^{(D)}_{\{1,0\},\{1,0\},\{1,0\}} = \frac{1}{\pi^d}\int\int \frac{d^dk_1 d^dk_2}{k_1^2(k_1-k_2)^2(k_2-p)^2} \tag{67}$$

this is converted into TSIL notation by $\mathbf{S}(x,y,z) = a^2\mathbf{J}^{(D)}_{\{1,\sqrt{x}\},\{1,\sqrt{y}\},\{1,\sqrt{z}\}}$ so that I can expand the integral into a finite plus divergent piece as

$$\begin{aligned}\mathbf{S}(x,y,z) =& S(x,y,z) - \frac{(x+y+z)}{2\epsilon^2} + \left[A(x)+A(y)+A(z)-(x+y+z)/2+s/4\right]/\epsilon \\ &+ A_\epsilon(x)+A_\epsilon(y)+A_\epsilon(z)+\mathcal{O}(\epsilon)\end{aligned} \tag{68}$$

where $S(x,y,z)$ is the finite piece. For the massless case we are dealing with here is simply

$$\mathbf{S}(0,0,0) = S(0,0,0)+\frac{s}{4\epsilon}+\mathcal{O}(\epsilon) \tag{69}$$

where $s = -p^2$ with the Euclidean or metric with signiture $(-+++)$[2]. We can simply this further since $S(0,0,0)$ has a particularly simple integrated form [10]

$$S(0,0,0) = \frac{13s}{8} - \frac{s}{2}\log\left(\frac{-s}{Q^2}\right) \tag{70}$$

so we have

$$\mathbf{S}(0,0,0) = \frac{13s}{8} - \frac{s}{2}\log\left(\frac{-s}{Q^2}\right) + \frac{s}{4\epsilon} + \mathcal{O}(\epsilon) \tag{71}$$

The notation used by Grozin makes use of the basis integrals G_1 and G_2 given by

$$G_1 = -\frac{2g_2}{(d-3)(d-4)} G_2 = \frac{4g_2}{(d-3)(d-4)(3d-8)(3d-10)} \tag{72}$$

where

$$g_n = \frac{\Gamma(1+n\epsilon)\Gamma^(n+1)(1-\epsilon)}{\Gamma(1-(n+1)\epsilon)} \tag{73}$$

although Grozin provides a general form for G_n it is apparently incorrect, the lack of explanation for his notation renders it useless (one can attempt to infer what the subscripts on the brackets mean, but even the most creative explanations will not give a result consistent with G_1 and G_2 as stated elsewhere in the paper).

The Gamma function is expanded by Grozin to be

$$\Gamma(1+\epsilon) = \exp\left[-\gamma\epsilon + \sum_{n=2}^{\infty} \frac{(-1)^n \zeta_n}{n} \epsilon^n\right] \tag{74}$$

where $\zeta_n = \sum_{k=1}^{\infty} 1/k^n$ is the Riemann ζ function ($\zeta_2 = \pi^2/6$).

3.3.2 Integrated results

We will use the analytic expressions for the fully integrated amplitudes from Sato [7]. These are

$$\Sigma_{f,1} = \frac{e_f^4 \not{p}}{(16\pi^2)^2}\left[\frac{1}{\epsilon^2} + \frac{2}{2\epsilon} + \frac{21}{4} - \zeta_2\right]\left(-\frac{p^2}{Q^2}\right)^{-2\epsilon} + \mathcal{O}(\epsilon) \tag{75}$$

$$\Sigma_{f,2} = \frac{e_f^4 \not{p}}{(16\pi^2)^2}\left[-\frac{1}{2\epsilon^2} - \frac{5}{4\epsilon} - \frac{31}{8} + \frac{\zeta_2}{2}\right]\left(-\frac{p^2}{Q^2}\right)^{-2\epsilon} + \mathcal{O}(\epsilon) \tag{76}$$

$$\Sigma_{f,3} = \sum_{f'} \frac{e_f^2 e_{f'}^2 \not{p}}{(16\pi^2)^2}\left[-\frac{1}{\epsilon} - \frac{7}{2}\right]\left(-\frac{p^2}{Q^2}\right)^{-2\epsilon} + \mathcal{O}(\epsilon) \tag{77}$$

[2]Note that in the Mass Builder Mathematica package where this expansion is implemented, I take $s = p^2$ as the p^2 inserted here at evaluation time is positive.

which I express in a proper expansion of ϵ as

$$\Sigma_{f,1} = \frac{e_f^4 \not{p}}{(16\pi^2)^2}\left[\frac{1}{\epsilon^2}+\frac{1}{\epsilon}\left(\frac{3}{2}-2\log\left(-\frac{p^2}{Q^2}\right)\right)+\left(2\log^2\left(-\frac{p^2}{Q^2}\right)-3\log\left(-\frac{p^2}{Q^2}\right)-\zeta+\frac{21}{4}\right)\right]+\mathcal{O}(\epsilon) \tag{78}$$

$$\Sigma_{f,2} = \frac{e_f^4 \not{p}}{(16\pi^2)^2}\left[-\frac{1}{2\epsilon^2}+\frac{1}{\epsilon}\left(-\frac{5}{4}+\log\left(-\frac{p^2}{Q^2}\right)\right)+\frac{1}{8}\left(-8\log^2\left(-\frac{p^2}{Q^2}\right)+20\log\left(-\frac{p^2}{Q^2}\right)+4\zeta-31\right)\right]+\mathcal{O}(\epsilon) \tag{79}$$

$$\Sigma_{f,3} = e^4\left[-\frac{1}{\epsilon}+\left(2\log\left(\frac{p^2}{Q^2}\right)-\frac{7}{2}\right)\right]+\mathcal{O}(\epsilon) \tag{80}$$

3.3.3 Diagram 3

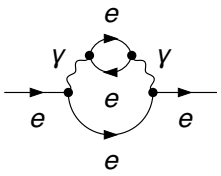

The first two-loop diagram we consider is given on the left. I find consistency between my result and that of FeynHelpers, Sato and Grozin. The integral is given by [7]

$$\Sigma_{f,3} = e^4(\mu^{4-d})^2\int\frac{d^dk}{(2\pi)^d}\frac{d^dk'}{(2\pi)^d}\frac{\gamma_\mu(\not{k}-\not{p})\gamma_\nu}{(k^2)^2(k-p)^2}\frac{\mathrm{Tr}[\gamma^\mu\not{k}'\gamma^\nu(\not{k}'-\not{k})]}{k'^2(k'-k)^2} \tag{81}$$

The UV divergent amplitude given by an intermediate step in the Mass Builder algorithm is

$$\Sigma_{f,3} = e^4\frac{2(d-2)^2}{(d-6)p^2}\mathbf{J}^{(D)}_{\{1,0\},\{1,0\},\{1,0\}} \tag{82}$$

The amplitude given by FeynHelpers is in agreement, using the Mathematica example code available with the package [8]. To get the FeynHelpers result in an equivalent form we apply the steps

```
In[1]:= tfiamp = resSE // ToTFI[#, l1, l2, p] &;
        SE = Simplify[TarcerRecurse[tfiamp]]
```

which does not alter the result but expresses it in terms of TARCER integrals for the sake of comparison. I expand this result into a fully integrated divergent form to be

$$\Sigma_{f,3} = e^4\left[-\frac{1}{\epsilon}+\left(2\log\left(\frac{p^2}{Q^2}\right)-\frac{7}{2}\right)\right]+\mathcal{O}(\epsilon) \tag{83}$$

this agrees exactly with (80).

We next compare this with Grozin's result

$$\Sigma_{f,3} = e^4 \frac{(-p^2)^{-2\epsilon}}{(4\pi)^d} G_2 \frac{2(d-2)^2}{(d-6)} \tag{84}$$

which is expanded to give

$$\Sigma_{f,3} = -e^4 \left[-\frac{1}{\epsilon} + \left(2\gamma + 2\log\left(\frac{p^2}{Q^2}\right) - \frac{7}{2} \right) \right] + \mathcal{O}(\epsilon) \tag{85}$$

which is in agreement with (80) except for the γ term, which I will discuss later (scheme dependent term I expect?).

3.3.4 Diagram 2

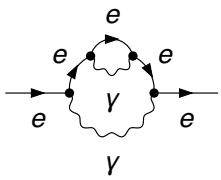

The next two-loop diagram we consider is given on the left. The integral for this amplitude is

$$\Sigma_{f,2} = e^4 (\mu^{4-d})^2 \int \frac{d^d k}{(2\pi)^d} \frac{d^d k'}{(2\pi)^d} \frac{\gamma_\mu \not{k} \gamma^\nu \not{k}' \gamma_\nu \not{k} \gamma_\mu}{(k^2)^2 (k'^2)^2 (p-k)^2 (k-k')^2} \tag{86}$$

The result from Grozin is

$$\Sigma_{f,2} = e^4 \frac{(-p^2)^{-2\epsilon}}{(4\pi)^d} G_2 \frac{(d-2)^2(d-3)}{(d-4)} \tag{87}$$

which is expanded to give

$$\begin{aligned} \Sigma_{f,2} =& e^4 \left[-\frac{1}{2\epsilon^2} + \frac{1}{\epsilon} \left(\frac{5}{4} - \gamma - \log\left(\frac{p^2}{Q^2}\right) \right) \right. \\ & \left. + \frac{1}{8} \left(31 + 4\gamma(2\gamma - 5) - 4\zeta + 4\log\left(\frac{p^2}{Q^2}\right) \left(4\gamma + 2\log\left(\frac{p^2}{Q^2}\right) - 5 \right) \right) \right] + \mathcal{O}(\epsilon) \end{aligned} \tag{88}$$

this agrees with (79).
The UV divergent amplitude given by an intermediate step in the Mass Builder algorithm is

$$\Sigma_{f,2} = e^4 \frac{(d-3)(d-2)^2}{(d-4)p^2} p \, \mathbf{J}^{(D)}_{\{1,0\},\{1,0\},\{1,0\}} \tag{89}$$

which agrees with the FeynHelpers result. Expanding this out using (71) gives

$$\Sigma_{f,2} = e^4 \left[-\frac{1}{2\epsilon^2} + \frac{1}{\epsilon} \left(\log\left(\frac{p^2}{Q^2}\right) - \frac{5}{4} \right) + \left(\frac{21}{2} - 4\log\left(\frac{p^2}{Q^2}\right) \right) \right] + \mathcal{O}(\epsilon) \tag{90}$$

which is in disagreement with (79). This is because (79) does not include $\mathcal{O}(\epsilon)$ terms, which become relevant in this amplitude due to $\mathcal{O}(1/\epsilon)$ terms in the coefficient of the basis integral. So to get a consistent result we augment the code to include these terms, which will only become relevant in this massless case. So in Mass Builder we now define

$$\begin{aligned}\mathbf{S}(0,0,0) = &\frac{s}{4\epsilon} + \frac{13s}{8} - \frac{s}{2}\log\left(\frac{-s}{Q^2}\right) \\ &+ \epsilon\frac{s}{16}\left[-4\zeta + 115 + 8(\log(-\frac{s}{Q^2}))^2 - 52\log(-\frac{s}{Q^2})\right] + \mathcal{O}(\epsilon^2)\end{aligned} \tag{91}$$

3.3.5 Diagram 1

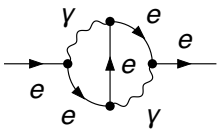

The final two-loop diagram we consider is given on the left. Section not yet completed. The understanding gained from above is sufficient to complete the calcuation, the result of this diagram is analogous.

3.4 Counter-terms and cancellation of divergences

In this section I calculate the counter-term diagrams and determine the required counter-term couplings for a model where the masses are zero from the beginning (as in the calculation above) and one where we include regulator masses for all fields. We present result below for the case with masses for the fermion and vector fields, m_f and m_a respectively.

3.4.1 Counter-term diagram 1

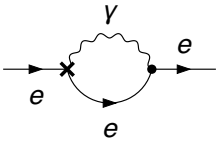

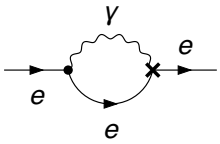

The first two counter-term diagrams I consider are given on the left. The counter-term coupling for the vertex here is taken from [7], and is the only counter-term that we can not determine ourself. This is

$$\delta_1 = -e^2 \tag{92}$$

The counter-term diagrams on the left cancel logarithmic divergences from diagram 1 considered above. Such that the sum of these two diagrams and diagram one is

$$D_1 = \frac{e^4}{(16\pi^2)^2}\left[\frac{1}{\epsilon^2}(4m_f - p) + \frac{1}{\epsilon}(12m_f - p)\right] + \mathcal{O}(\epsilon^0) \tag{93}$$

δ_1	$\delta_z^{(1,1)}$	$\delta_m^{(1,1)}$	$\delta_{3,z}$	$\delta_{3,m}$	$\delta_m^{(2,1)}$	$\delta_z^{(2,1)}$	$\delta_m^{(2,2)}$	$\delta_z^{(2,2)}$
Massive QED								
$-e^2$	$-e^2$	$4e^2$	$\frac{4}{3}e^2$	0	$\frac{8}{3}e^4 m_f$	$\frac{7}{4}e^4$	$\frac{6}{3}e^4 m_f$	$\frac{1}{2}e^4$
Massless QED								
e^2	$-e^2$	0	$\frac{4}{3}e^2$	0	0	$\frac{7}{4}e^4$	0	$\frac{1}{2}e^4$

Table 1: The counter-term couplings required for a divergence free amplitude in the case of massless and massive QED. The only non-trivial difference between the models is for δ_1 where the sign is opposite.

3.4.2 Counter-term diagram 2

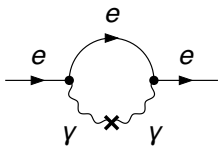

The counter-term diagram on the left cancels logarithmic divergences from diagram 3 considered above. The counter-term coupling is determined at one-loop and is given in Table 1. The sum of this diagram and diagram 3 is

$$D_2 = \frac{e^4}{(16\pi^2)^2}\left[-\frac{2}{\epsilon^2}m_f + \frac{1}{3\epsilon}(8m_f - 3p)\right] + \mathcal{O}(\epsilon^0) \tag{94}$$

3.4.3 Counter-term diagram 3

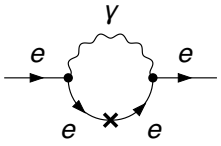

The counter-term diagram on the left cancels logarithmic divergences from diagram 2 considered above. The counter-term coupling is determined at one-loop and is given in Table 1. The sum of this diagram and diagram 3 is

$$D_3 = \frac{e^4}{(16\pi^2)^2}\left[\frac{1}{\epsilon^2}(8m_f + p) - \frac{1}{4\epsilon}(24m_f + p)\right] + \mathcal{O}(\epsilon^0) \tag{95}$$

The sum of the left over divergences above must be cancelled by the tree-level counter-term coupling, which is

$$\Sigma_1^{(1c)} = \kappa\left[\frac{1}{\epsilon}\left(\delta_m^{(1,1)} + \not{p}\delta_z^{(1,1)}\right)\right] + \kappa^2\left[\frac{1}{\epsilon}\left(\delta_m^{(2,1)} + \not{p}\delta_z^{(2,1)}\right) + \frac{1}{\epsilon^2}\left(\delta_m^{(2,2)} + \not{p}\delta_z^{(2,2)}\right)\right] \tag{96}$$

which is easily solved to cancel the divergences in D_1, D_2 and D_3. The solutions are given in Table 1.

4 The electroweak triplet model

4.1 Introduction

The extension of the standard model by an electroweak multiplet is a popular dark matter candidate theory. At the lowest order in perturbation theory all components of the multi-

plet have the same mass, which would result in charged dark matter, contrary to what is observed. However when one goes to the next order in perturbation theory by computing the radiatively corrected mass, then the charged component(s) will obtain a slightly larger mass correction than the neutral component, resulting in a sufficient mass splitting to render the charged components to have a lifetime much shorter than the age of the universe. The exact value of this mass splitting at the two-loop level is of interest. We will work with the most simple multiplet, an $SU(2)$ triplet, to determine the value of this mass splitting at the two-loop order in perturbation theory.

To further reduce the number of interactions we need to consider we will use a simplified standard model with the most minimal components to achieve a mass splitting. This model consists of the $U(1)$ and $SU(2)$ gauge sectors but no SM fermions or leptons. The particle content of the model is given in Table 2. The triplet sector of the Lagrangian is

$$\begin{aligned}\mathcal{L}_\chi =& \frac{1}{2}\overline{\chi^0}(i\not{\partial} - m_\chi)\chi^0 + \frac{1}{2}\overline{\chi^+}(i\not{\partial} - m_\chi)\chi^+ \\ &+ g\left(\overline{\chi^+}\gamma_\mu\chi^+\right)(s_W A_\mu + c_W Z_\mu) \\ &+ g\left(\overline{\chi^+}\gamma_\mu\chi^0\right)W_\mu^+ + \text{h.c.}\end{aligned} \tag{97}$$

where $s_W = \sin(\theta_W)$ and $c_W = \cos(\theta_W)$ are the sine and cosine of the Weinberg angle respectively.

The Higgs sector is given by

$$\mathcal{L}_H = \mu^2\overline{H}H - \lambda(\overline{H}H)^2 \tag{98}$$

The mixing in the gauge sector after EWSB is given by

$$\begin{pmatrix} B_\rho \\ W_{3\rho} \end{pmatrix} = Z^{\gamma Z}\begin{pmatrix} \gamma_\rho \\ Z_\rho \end{pmatrix} \tag{99}$$

$$\begin{pmatrix} W_{1\rho} \\ W_{2\rho} \end{pmatrix} = Z^{W}\begin{pmatrix} W_\rho^+ \\ W_\rho^+ \end{pmatrix} \tag{100}$$

$$\tag{101}$$

where the mixing matrices are parametrised by

$$Z^{\gamma Z} = \begin{pmatrix} c_W & -s_W \\ s_W & c_W \end{pmatrix} \tag{102}$$

$$Z^{W} = \frac{1}{\sqrt{2}}\begin{pmatrix} 1 & 1 \\ i & -i \end{pmatrix}. \tag{103}$$

$$\tag{104}$$

The gauge fixing sector has Lagrangian in the gauge eigenstate

$$L_{GF} = -\frac{1}{2}|\partial_\mu B|^2\xi_B^{-1} - \frac{1}{2}|\partial_\mu W|^2\xi_W^{-1} \tag{105}$$

and in the EWSB eigenstate

$$L_{GF} = -\frac{1}{2}A^0 v\xi_Z\Big(g_1\sin\Theta_W + g_2\cos\Theta_W\Big) + \partial_\mu Z|^2\xi_Z^{-1} - \frac{1}{2}|\partial_\mu\gamma|^2\xi_\gamma^{-1} \tag{106}$$

$$-\frac{i}{2}g_2 H^+ v\xi_{W^+} + \partial_\mu W^+|^2\xi_{W^+}^{-1}. \tag{107}$$

In our choice of gauge the ghost fields take on the same mass as their respective field, such that $m_{\eta_\gamma} = m_\gamma$, $m_{\eta_Z} = m_Z$, $m_{\eta^+} = m_W$. This is true only in the Feynman-'t Hooft gauge, see here.

The fields A_0 and H^+ are also given masses of $m_{A_0} = m_Z$ and $m_{H^+} = m_W$.
I don't understand how the Goldstone bosons can have the same mass as the physical gauge bosons. From what I can understand, initially when we write the theory down the Goldstone bosons are scalar fields and the gauge bosons are massless vector fields. Then the degree of freedom from the Goldstone bosons can be used as a mass degree of freedom for the gauge bosons. So the Goldstone bosons are no longer a degree of freedom, they disappear. So I don't understand how we can have massive Goldstone bosons and massive gauge bosons. Even if somehow this works, these are the gauge bosons before we do the mixing to obtain Z and A, rather than B and W_3, so I don't get how the masses can correspond so nicely. Obviously it does work, because the 1-loop gauge boson self energies I have calculated come out exactly as expected, and there are diagrams containing these Goldstone bosons involved. However, I have no idea how this works.

We use the following relationships in the input to Mass Builder, to reduce the number of free variables required at run time

$$\begin{aligned} s_W^2 &= \frac{g_1^2}{g_1^2+g_2^2}, & c_W^2 &= \frac{g_2^2}{g_1^2+g_2^2} \\ \alpha &= \frac{g_1^2 g_2^2}{g_1^2+g_2^2}, & v &= \frac{2m_W}{g_2}, \quad \alpha = e^2 \end{aligned} \tag{108}$$

The momentum dependent contribution to the triplet mass, the self energy, is given by calculating the 1PI loop process. For the χ^0 at one loop level this involves a loop with a W boson and $\chi^\pm$ particle, for $\chi^\pm$ we also have loops involving $\chi^{\pm\pm}$, $W^\pm$ and the A and Z

Table 2: The particle content of the electroweak triplet model.

Name	Type	complex/real	Mass
H^+	Scalar	complex	m_W
A^0	Scalar	real	m_Z
h	Scalar	real	m_H
χ^+	Fermion	Dirac	m_χ
χ_0	Fermion	Majorana	m_χ
γ	Vector	real	m_γ
Z	Vector	real	m_Z
W^+	Vector	complex	m_W
η^γ	Ghost	real	m_γ
η^Z	Ghost	real	m_Z
η^+	Ghost	complex	m_W
η^-	Ghost	complex	m_W

bosons. The propagators we will use are (in the Feynman gauge)

$$i\Pi^V_{\mu\nu} = -i\frac{-g_{\mu\nu}}{k^2 - m_V^2 - \Pi(k^2)} \tag{109}$$

$$i\Pi^\chi_{\mu\nu} = -i\frac{\not{k} - m_\chi}{k^2 - m_\chi^2 - \Pi(k^2)} \tag{110}$$

for the vector bosons ($V \in \{W^\pm, \gamma, Z\}$) and the components of the fermionic triplet ($\chi \in \{\chi^0, \chi^\pm\}$).

Because there is a large number of possible couplings and particles in this theory we use SARAH [11] to generate the FeynArts [3] model file rather than listing these by hand. The SARAH model file is given in section C.

The aim of this section is to the compute the full two-loop self energy of the charged and neutral components of the electroweak triplet, χ. For this we will require the one-loop self energy, the derivative of the one-loop self energy and the two-loop self energy. To obtain the necessary contributions from the two-loop order counter-terms we will also require the counter-term couplings involved. For this theory, these are limited to the tree-level counter-term couplings for the gauge bosons and the triplet, along with a single vertex correction. All these quantities will be presented in the remainder of this section.

4.1.1 Pole mass calculation

We present here a detailed discussion of the method of pole mass calculation in the electroweak triplet theory. The pole mass is obtained from the 1PI effective two-point function,

$$\Gamma_2 = \not{p} - M_0 + \Sigma_K(p^2)\not{p} + \Sigma_M(p^2) \tag{111}$$

where p is the four momentum of the particle and M_0 is the tree-level (or MS-bar after renormalisation) mass, and $\Sigma(p^2) = \Sigma_M(p^2) + \not{p}\Sigma_K(p^2)$ is the self energy. The pole mass is obtained by demanding $\Gamma_2 = 0$ which can be achieved by setting $p = \not{p} = M_{\rm pole}$ and iterating

$$M_{\rm pole} = \mathrm{Re}\left[\frac{M_0 - \Sigma_M(M^2_{\rm pole})}{1 + \Sigma_K(M^2_{\rm pole})}\right]. \tag{112}$$

This is the first of two methods to calculate the pole mass, which we will refer to as $M_{{\rm pole},A}$ or the *implicit pole mass*.

Alternatively (112) can be expanded as a power series in the gauge coupling g, where for each self energy function we have $\mathcal{O}(\Sigma^{(n)}) = \mathcal{O}(g^{2n})$ where n is the number of radiative loop corrections computed for the self energy function. First, expressing the self energies as a power series in g we have

$$M_{\rm pole} = \mathrm{Re}\left[\frac{M_0 - \Sigma^{(1)}_M(M^2_{\rm pole}) - \Sigma^{(2)}_M(M^2_{\rm pole}) + \mathcal{O}(g^6)}{1 + \Sigma^{(1)}_K(M^2_{\rm pole}) + \Sigma^{(2)}_K(M^2_{\rm pole}) + \mathcal{O}(g^6)}\right] \tag{113}$$

Then using a Taylor expansion we find to order g^6

$$\begin{aligned} M_{\rm pole} = M_0 - \Sigma^{(1)}_M - \Sigma^{(2)}_M - M_0\Sigma^{(1)}_K + \Sigma^{(1)}_M\Sigma^{(1)}_K \\ -M_0\Sigma^{(2)}_K + \Sigma^{(1)}_K\Sigma^{(1)}_K + \mathcal{O}(g^6)\Big|_{p^2=M^2_{\rm pole}} \end{aligned}$$

where $\Sigma^{(n)}_X = \Sigma^{(n)}_X(p^2)$ such that p^2 is the first argument in the two point functions appearing in the self energies. However, this is still an iterative expression, to get an expression without iterating we must change p here from $M_{\rm pole}$ to M_0.

Demanding that the self energies are evaluated at the tree level mass requires the use of the Taylor expansion,

$$\begin{aligned} &\Sigma^{(1)}_M\Big|_{p^2=M^2_{\rm pole}} = \\ &\Sigma^{(1)}_M + 2M_0(M_{\rm pole} - M_0)\dot{\Sigma}^{(1)}_M + \mathcal{O}\left(g^6\right)\Big|_{p^2=M_0^2}. \end{aligned} \tag{114}$$

However this is not yet an explicit expression for $M_{\rm pole}$, so we use the relation

$$\begin{aligned} M_{\rm pole} - M_0 &= -M_{\rm pole}\Sigma_K^{(1)}(M_{\rm pole}^2) - \Sigma_M^{(1)}(M_{\rm pole}^2) + \mathcal{O}(g^4) \\ &= -M_{\rm pole}\Sigma_K^{(1)}(M_0) - \Sigma_M^{(1)}(M_0) + \mathcal{O}(g^4) \end{aligned} \tag{115}$$

which comes directly from demanding (111) be equal to zero, and the second line follows from using (114) to discard higher order terms. An error of order g^4 is acceptable for this difference since it appears in the final expression as the coefficient of the term $\dot{\Sigma}_K^{(1)}$ and thus will be a total error of order g^6. Finally, to remove the $M_{\rm pole}$ on the right-hand side we use the same expression within itself (effectively iterating)

$$\begin{aligned} M_{\rm pole} - M_0 &= -M_{\rm pole}\Sigma_K^{(1)}(M_0) - \Sigma_M^{(1)}(M_0) + \mathcal{O}(g^4) \\ &= -M_0\Sigma_K^{(1)}(M_0) - \Sigma_M^{(1)}(M_0) + \mathcal{O}(g^4) \end{aligned} \tag{116}$$

substituting this result into (114) gives

$$\begin{aligned} &\Sigma_M^{(1)}\Big|_{p^2=M_{\rm pole}^2} = \\ &\Sigma_M^{(1)} - 2M_0(M_0\Sigma_K^{(1)} + \Sigma_M^{(1)})\dot{\Sigma}_M^{(1)} + \mathcal{O}\left(g^6\right)\Big|_{p^2=M_0^2}. \end{aligned} \tag{117}$$

For the two loop corrections we need not compute the details of the derivative term, since we already know it will be above order g^6 so we simply use

$$\Sigma_M^{(2)}\Big|_{p^2=M_{\rm pole}^2} = \Sigma_M^{(2)} + \mathcal{O}\left(g^4(M_{\rm pole} - M_0)^2\right)\Big|_{p^2=M_0^2}.$$

Similar relations hold for $\Sigma_K^{(1)}$ and $\Sigma_K^{(2)}$.

With the use of these expressions we can express (113) with all functions evaluated at M_0 to give

$$\begin{aligned} M_{\rm pole} = \Big[&M_0 - \Sigma_M^{(1)} - \Sigma_M^{(2)} - M_0\Sigma_K^{(1)} - M_0\Sigma_K^{(2)} \\ &+ (\Sigma_M^{(1)} + M_0\Sigma_K^{(1)})(\Sigma_K^{(1)} + 2M_0\dot{\Sigma}_M^{(1)} + 2M_0^2\dot{\Sigma}_K^{(1)}) \\ &+\mathcal{O}\left(g^6\right)\Big]_{p^2=M_0^2} \end{aligned} \tag{118}$$

which agrees with Ibe and Sato [2]. Reducing this to the one-loop level we obtain

$$M_{\rm pole} = \left[M_0 - \Sigma_M^{(1)} - M_0\Sigma_K^{(1)} + \mathcal{O}\left(g^4\right)\right]_{p^2=M_0^2} \tag{119}$$

which is the second method of pole mass calculation we will use, we refer to this as $M_{{\rm pole},B}$ or the *explicit pole mass*.

In summary, we have derived an explicit expression for the pole mass by invoking the perturbativity of the gauge coupling. These two methods will be used to compute the two-loop pole mass of the triplet particles.

4.2 One-loop self energies

In this section we compute all the required one-loop self energies of the particles in the electroweak triplet theory. Along with the one-loop self energy of triplet itself we must also compute the one-loop self energies of the bosons which appear in this calculation. This is because these internal boson propagators can have counter-terms inserted and thus become of two-loop order, so we will need to evaluate what these counter-term couplings are.

To compute the counter-terms for the gauge boson propagators we must compute the one-loop self energies and demand that these are free of UV divergences. The computation of these one-loop self energies, which involve all the ghost and pre-EWSB scalar states, is also a good opportunity to check the model is consistent with similar results in the literature. The analytic form for these amplitudes is presented in Ibe et al. [2] along with the counter-term which we can make a direct comparison.

Therefore we will present the details of the one-loop contributions to the amplitude, $\Pi(p^2)$, appearing in the gauge boson propagators, (109), for each boson we require. These contributions are given by

$$\Pi_{V_1V_2} = \Pi^{(V,h)}_{V_1V_2} + \Pi^{(\tilde{\chi})}_{V_1V_2} + p^2\delta_{Z_{V_1V_2}} + \delta_{m^2_{V_1V_2}} \ , \tag{120}$$

where $V_1V_2 = \gamma\gamma$, γZ, ZZ, and WW. The first term in the right-hand side is the contributions from the gauge-Higgs sector of the SM and the second term is from the electroweak triplet. The third and fourth terms are the one-loop counter-terms which are determined by demanding no UV divergences in the total $\Pi_{V_1V_2}$.

We do not need to consider the one-loop self energies of the Higgs, ghosts, or pre-EWSB bosons as these do not appear in the one-loop triplet self energies. Thus we do not need to determine the counter-terms which would be of two-loop order. However, if we wanted to compute a three-loop self energy, these would then be required as their propagators appear in the two-loop triplet self energy.

4.2.1 Triplet neutral component

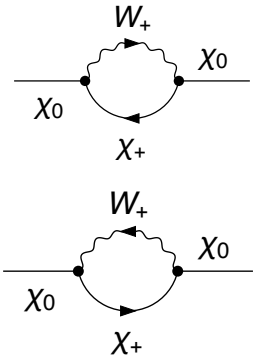

The neutral component only has two possible radiative corrections, due to the processes $\chi_0 \to W^{\pm} + \chi^{\mp}$. The corresponding Feynman diagrams are given on the left. The loop integral we need to evaluate is

$$i\Sigma_{\chi^0}(\not{p}) = 2(g)^2 \int \frac{\mathrm{d}^4 k}{(2\pi)^4} \gamma^{\mu} \frac{(\not{p} + \not{k} + m_{\chi})\gamma^{\nu}\,(-g_{\mu\nu})}{((p+k)^2 - m_{\chi}^2)(k^2 - m_W^2)} \tag{121}$$

where we have included a factor of two since this process can occur via either $\chi_0 \to W^+ + \chi^-$ or $\chi_0 \to W^- + \chi^+$.

We will calculate the neutral component self energy by hand for the purposes of illustration and leave the rest of the calculations to the tools we have available. The loop integral is expressed as

$$i\Sigma_{\chi^0}(\not{p}) = 2(g)^2 \int \frac{\mathrm{d}^4 k}{(2\pi)^4} \frac{N}{((p+k)^2 - m_{\chi}^2)(k^2 - m_W^2)} \tag{122}$$

where we simplify N by

$$\begin{aligned} N &= -\gamma^{\mu}(\not{k} + \not{p} + m_{\chi})\gamma^{\nu} g_{\mu\nu} \\ &= -\gamma^{\mu}(\not{k} + \not{p} + m_{\chi})\gamma_{\mu} \\ &= (D-2)(\not{k} + \not{p}) - D m_{\chi} \end{aligned}$$

using the identities

$$\begin{aligned} \gamma_{\mu}\not{a}\gamma^{\mu} &= (2-D)\not{a} \\ \gamma^{\mu}\gamma_{\mu} &= DI \end{aligned} \tag{123}$$

where I is the identity matrix in D dimensions.

Now we use the Feynman parameter integral

$$\frac{1}{AB} = \int_0^1 \frac{\mathrm{d}x}{[A + (B-A)x]^2} \tag{124}$$

to simplify the denominator

$$\begin{aligned}\frac{1}{((p+k)^2-m_\chi^2)(k^2-m_W^2)} &= \int_0^1 \frac{\mathrm{d}x}{[k^2-m_W^2+(p^2+2kp+k^2-(k^2-m_W^2))x]^2} \\ &= \int_0^1 \frac{\mathrm{d}x}{[k^2+2kpx+p^2x+x(m_W^2-m_\chi^2)-m_W^2]^2} \\ &= \int_0^1 \frac{\mathrm{d}x}{[(k+px)^2+x(1-x)p^2+x(m_W^2-m_\chi^2)-m_W^2]^2} \\ &= \int_0^1 \frac{\mathrm{d}x}{[k'-\xi]^2}\end{aligned}$$

where $k' = k + px$ and we have defined $\xi \equiv -x(1-x)p^2 - x(m_W^2 - m^2) + m_W^2$. Note that we choose $(p+k)$ for the momentum in the χ internal propagator, this is to match the convention used by Ibe et al. [2] and thus the definitions for the Passarino-Veltman integrals we will make use of shortly.

We now translate the integration measure $\int \mathrm{d}^4k \to \int \mathrm{d}^4k'$ (and henceforth omitting the prime on k') to obtain (after substituting $k \to k - px$ in the numerator)

$$i\Sigma_{\chi^0}(\not{p}) = 2(g)^2 \int \frac{\mathrm{d}^4k}{(2\pi)^4} \int_0^1 \mathrm{d}x \frac{(D-2)(\not{k}+\not{p}(1-x)) - Dm_\chi}{[k^2-\Delta]^2}. \tag{125}$$

Since the denominator of the loop integral is now symmetric with respect to k we can discard all terms here of odd order in k to give

$$i\Sigma_{\chi^0}(\not{p}) = 2(g)^2 \int \frac{\mathrm{d}^4k}{(2\pi)^4} \int_0^1 \mathrm{d}x \frac{(D-2)(1-x)\not{p} - Dm_\chi}{[k^2-\Delta]^2}. \tag{126}$$

Next we apply dimensional regularisation, letting $D = 4 - 2\epsilon$, such that in the limit of small ϵ we have

$$\begin{aligned}\int \frac{\mathrm{d}^4k}{(2\pi)^4}[k^2-\Delta]^{-2} &\to \mu^{2\epsilon} \int \frac{\mathrm{d}^Dk}{(2\pi)^D} \frac{1}{[k^2-\Delta]^2} \\ &= \mu^{2\epsilon} \frac{i}{(4\pi)^{\frac{D}{2}}} \frac{1}{\Delta^{2-\frac{D}{2}}} \Gamma\left(\frac{4-D}{2}\right) \\ &= \mu^{2\epsilon} \frac{-i}{(4\pi)^2} \frac{1}{\Delta^\epsilon} \Gamma(\epsilon)\,(4\pi)^\epsilon \\ &\approx \frac{i}{(4\pi)^2}(1-\epsilon\log\Delta)\left(\frac{1}{\epsilon}-\gamma\right)(1+\epsilon\log 4\pi)\left(1+\epsilon\log\mu^2\right) \\ &= \frac{i}{(4\pi)^2}\left(\frac{1}{\epsilon}-\gamma+\log\frac{4\pi\mu^2}{\Delta}\right)+\mathcal{O}(\epsilon).\end{aligned}$$

We are now ready to calculate the integral for $i\Sigma_{\chi^0}(\not{p})$. Setting $D = 4-2\epsilon$ in the numerator we have

$$i\Sigma_{\chi^0}(\not{p}) = 2(g)^2 \frac{i}{(4\pi)^2} \int_0^1 \mathrm{d}x \left((2-2\epsilon)(1-x)\not{p} - (4-2\epsilon)m_\chi\right) \left(\frac{1}{\epsilon} + \log\frac{4\pi\mu^2 e^{-\gamma}}{\Delta}\right). \quad (127)$$

After some simplification and evaluation of the straight forward integrals over x we find

$$i\Sigma_{\chi^0}(\not{p}) = 2(g)^2 \frac{i}{(4\pi)^2} \left[2m_\chi - \not{p} + 2\not{p}\left(-\frac{\Delta}{2} + \int_0^1 \mathrm{d}x\, x \log\frac{\xi}{\mu^2}\right)\right. \quad (128)$$

$$\left. + (2\not{p} - 4m_\chi)\left(\Delta - \int_0^1 \mathrm{d}x\, \log\frac{\xi}{\mu^2}\right)\right] \quad (129)$$

where we let $\Delta = 1/\epsilon - \gamma_E + \log(4\pi)$. Now using (158) and (159), following the definitions of Ibe et al. [2], we express this result in terms of Passarino-Veltman functions

$$i\Sigma_{\chi^0}(\not{p}) = \frac{-2i(g)^2}{(4\pi)^2}\left[2m - \not{p} + 2\not{p}\left(B_1(p^2, m_W^2, m_\chi^2)\right) + (2\not{p} - 4m_\chi)\left(B_0(p^2, m_W^2, m_\chi^2)\right)\right] \quad (130)$$

To bring this into the same form as given by Ibe et al. [2] we use the identities $B_1(p^2, m_1^2, m_2^2) = -B_1(p^2, m_2^2, m_1^2) - B_0(p^2, m_2^2, m_1^2)$ and $B_0(p^2, m_1^2, m_2^2) = B_0(p^2, m_2^2, m_1^2)$ such that

$$\Sigma_{\chi^0}(m) = \frac{g^2}{16\pi^2}\left[-m\left(8B_0(p^2, m_\chi^2, m_W^2) - 4\right) - \not{p}\left(4B_1(p^2, m_\chi^2, m_W^2) + 2\right)\right] \quad (131)$$

There is also a counter-term contribution, in the Figure on the left, with amplitude

$$\int \frac{\mathrm{d}^4k}{(2\pi)^4}\left(\not{p}\,\delta_{Z_{\tilde{\chi}}} - \delta_{m_{\tilde{\chi}}}\right) \quad (132)$$

The sum of these amplitudes gives the self energy $\Sigma_{\chi^0} = \Sigma^{(1)}_{m_\chi,0} + \not{p}\Sigma^{(1)}_{K,0}$ where

$$\Sigma^{(1)}_{K,0} = -\frac{g^2}{16\pi^2}\left[4B_1(p^2, m_\chi^2, m_W^2) + 2\right] + \delta_{Z_{\tilde{\chi}}}\ , \quad (133)$$

$$\Sigma^{(1)}_{m_\chi,0} = -\frac{g^2 m_\chi}{16\pi^2}\left[8B_0(p^2, m_\chi^2, m_W^2) - 4\right] - \delta_{m_\chi}\ . \quad (134)$$

Because we have used (158) and (159) to define B_0 and B_1 this result contains divergent terms and is only finite with the correct choice of the counter-term couplings which we will determine in section 4.3.

4.2.2 Triplet charged component

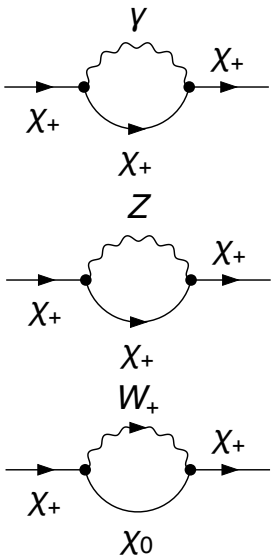

The charged component has three one-loop corrections with diagrams given on the left. The total amplitude for all three contributions is

$$\begin{aligned} i\Sigma_{\chi^-}(\not{p}) = &+ (s_W g)^2 \int \frac{\mathrm{d}^4k}{(2\pi)^4}\gamma^\mu \frac{(\not{p}-\not{k}+m_\chi)\gamma^\nu\,(-g_{\mu\nu})}{((p-k)^2-m_\chi^2)(k^2)} \\ &+ (g)^2 \int \frac{\mathrm{d}^4k}{(2\pi)^4}\gamma^\mu \frac{(\not{p}-\not{k}+m_\chi)\gamma^\nu\,(-g_{\mu\nu})}{((p-k)^2-m_\chi^2)(k^2-m_W^2)} \\ &+ (c_W g)^2 \int \frac{\mathrm{d}^4k}{(2\pi)^4}\gamma^\mu \frac{(\not{p}-\not{k}+m_\chi)\gamma^\nu\,(-g_{\mu\nu})}{((p-k)^2-m_\chi^2)(k^2-m_W^2)}. \end{aligned} \tag{135}$$

The calculation of these amplitudes is very similar to that for the neutral component, so we will not repeat the calculation. The result, obtained either using Mass Builder or by hand is

$$\Sigma^{(1)}_{K,\pm} = -\frac{g^2}{8\pi^2}\left[s_W^2 B_1(p^2,m_\chi^2,0) + c_W^2 B_1(p^2,m_\chi^2,m_Z^2) + B_1(p^2,m_\chi^2,m_W^2) + 1\right] + \delta_{Z_{\tilde{\chi}}} \tag{136}$$

$$\Sigma^{(1)}_{M,\pm} = -\frac{g^2 m_\chi}{4\pi^2}\left[s_W^2 B_0(p^2,m_\chi^2,0) + c_W^2 B_0(p^2,m_\chi^2,m_Z^2) + B_0(p^2,m_\chi^2,m_W^2) - 1\right] - \delta_{M_{\tilde{\chi}}} \tag{137}$$

where we have also included a counter-term contribution analogous to that in the neutral component calculation. These counter-terms $\delta_{Z_{\tilde{\chi}}}$ and $\delta_{M_{\tilde{\chi}}}$, are given in a later section.

4.2.3 Photon

Consider the contributions to the photon self energy from Higgs and boson sector.
From Ibe et al. we have

$$\Pi^{(V,h)}_{\gamma\gamma}(p^2) = -\frac{3e^2}{4\pi^2}\left[\tilde{B}_{22}(p^2,m_W^2,m_W^2) + \frac{p^2}{18}\right] - \frac{e^2p^2}{4\pi^2}B_0(p^2,m_W^2,m_W^2) \tag{138}$$

where this includes all contributions from the 9 diagrams in Figure 1. We find the self energy contribution from Mass Builder in a fully reduced scheme is

$$\Pi^{(V,h)}_{\gamma\gamma}(p^2) = \frac{\alpha}{32\pi^2}\left(\left(4m_W^2 - 6(2m_W^2+p^2)\right)B_0(m_W^2,m_W^2) + 8A_0(m_W^2) - 8m_W^2\right) \tag{139}$$

which is equivalent to (138) after using the tensor integral reduction relationships given in Appendix B.

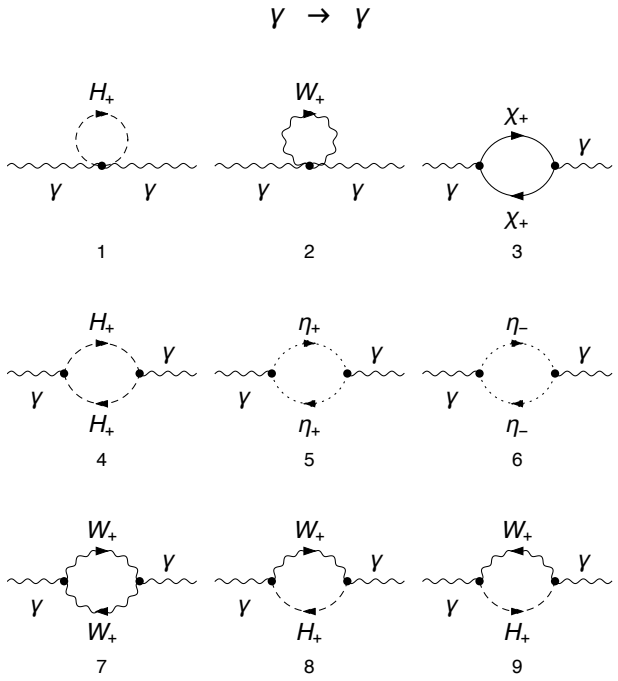

Figure 1: The one-loop corrections to the photon propagator.

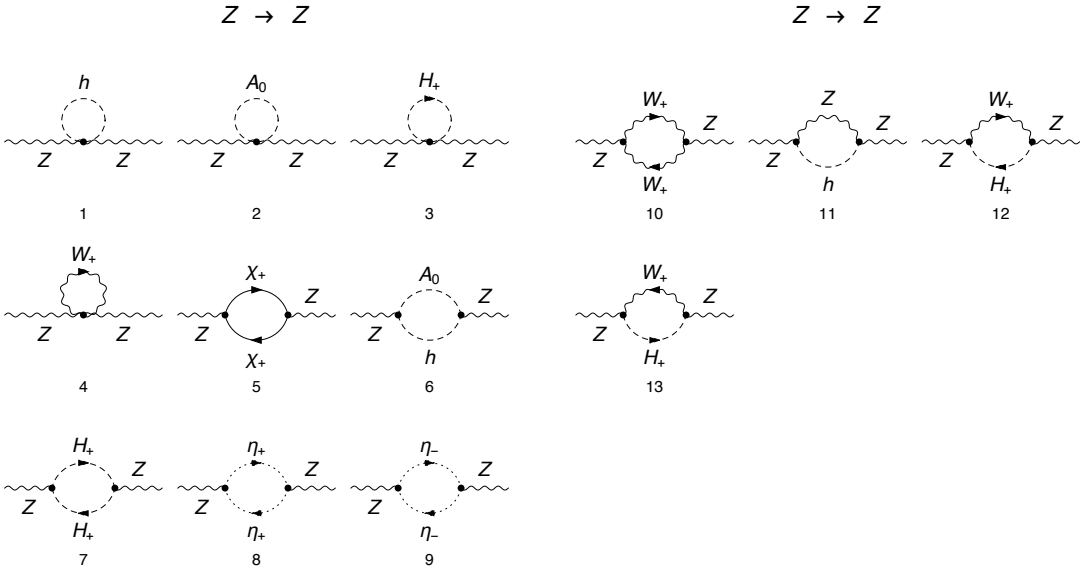

Figure 2: The one-loop corrections to the Z boson propagator.

4.2.4 Z boson

The Z boson self energy as given by Ibe et al. [2] is

$$\begin{aligned}\Pi_{ZZ}^{(V,h)}(p^2) &= -\frac{g^2(12c_W^4-4c_W^2+1)}{16\pi^2 c_W^2}\tilde{B}_{22}(p^2,m_W^2,m_W^2)-\frac{g^2c_W^2p^2}{24\pi^2}\\ &\quad -\frac{2g^2}{16\pi^2}(2c_W^2p^2+2m_W^2-m_Z^2)B_0(p^2,m_W^2,m_W^2)\\ &\quad -\frac{g^2}{16\pi^2c_W^2}[\tilde{B}_{22}(p^2,m_Z^2,m_H^2)-m_Z^2B_0(p^2,m_Z^2,m_H^2)] \qquad (140)\end{aligned}$$

the result from Mass Builder is

$$\begin{aligned}\Pi_{ZZ}^{(V,h)}(p^2) &= -\frac{g^2}{576c_W^4p^2\pi^2}\Big\{2p^2\Big[-3m_H^2(-1+s_W^2)+2p^2(1-3s_W^2+2s_W^4)\\ &\quad +3m_W^2(19-58s_W^2+64s_W^4-24s_W^6)\Big]\\ &\quad -3(m_W^2+m_H^2(-1+s_W^2)-2p^2(-1+s_W^2))A_0\left(m_H^2\right)\\ &\quad +12p^2(-9+29s_W^2-32s_W^4+12s_W^6)A_0\left(m_W^2\right)\\ &\quad +3((m_W^2+m_H^2(-1+s_W^2)+2p^2(-1+s_W^2))A_0\left(m_Z^2\right)\\ &\quad +\Big[-m_W^2(m_Z^2+10p^2)+m_H^4(-1+s_W^2)\\ &\quad +p^4(-1+s_W^2)+2m_H^2(m_W^2-p^2(-1+s_W^2))\Big]B_0\left(p^2,m_H^2,m_Z^2\right)\\ &\quad -p^2(-1+s_W^2)\Big[4m_W^2(15-32s_W^2+12s_W^4)\\ &\quad +p^2(39-76s_W^2+36s_W^4)\Big]B_0\left(p^2,m_W^2,m_W^2\right)\Big)\Big\} \qquad (141)\end{aligned}$$

which is equivalent to (140) after using the appropriate reduction relationships.

4.2.5 W boson

The W boson self energy is given by Ibe et al. [2] to be

$$\begin{aligned}\Pi_{WW}^{(V,h)}(p^2) &= -\frac{8e^2}{16\pi^2}\tilde{B}_{22}(p^2,0,m_W^2)-\frac{e^2p^2}{24\pi^2}-\frac{4e^2p^2}{16\pi^2}B_0(p^2,0,m_W^2)\\ &\quad -\frac{g^2}{16\pi^2}(1+8c_W^2)\tilde{B}_{22}(p^2,m_W^2,m_Z^2)-\frac{g^2c_W^2p^2}{24\pi^2}\\ &\quad -\frac{g^2}{16\pi^2}(4c_W^2p^2+3m_W^2-m_Z^2)B_0(p^2,m_W^2,m_Z^2)\\ &\quad -\frac{g^2}{16\pi^2}[\tilde{B}_{22}(p^2,m_W^2,m_H^2)-m_W^2B_0(p^2,m_W^2,m_H^2)]\ . \qquad (142)\end{aligned}$$

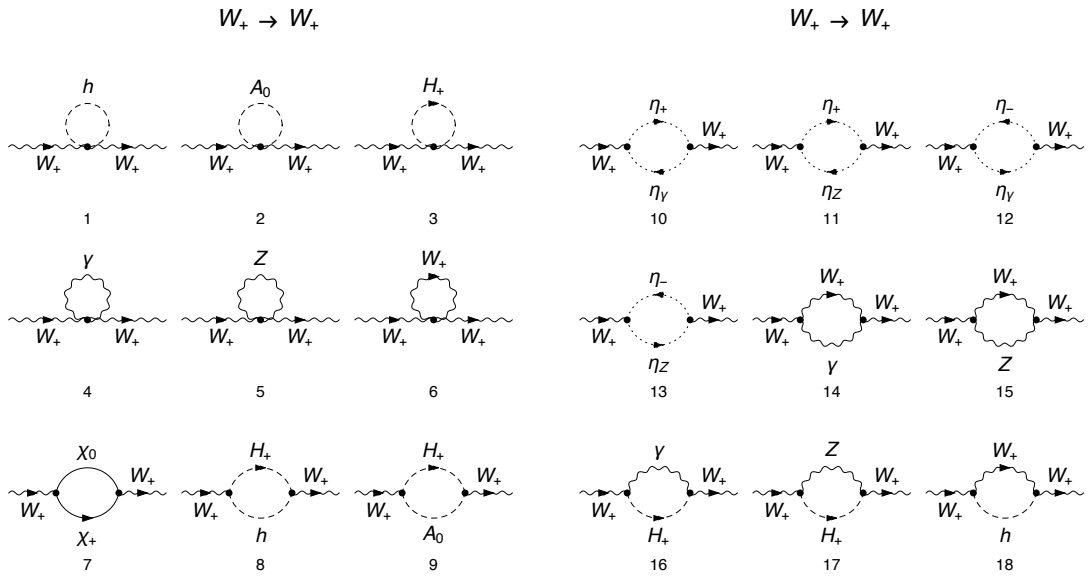

Figure 3: The one-loop corrections to the W boson propagator.

We compute the self energy using Mass Builder and obtain

$$
\begin{aligned}
\Pi^{(V,h)}_{WW}(p^2) \;=\; & -\frac{g^2}{576 c_W^4 p^2 \pi^2}\Big\{-6m_H^2p^2-4p^4+24(m_\gamma^2-m_W^2-2p^2)s_W^2(-1+s_W^2)A_0(m_\gamma^2)- \\
& 3m_H^2A_0(m_H^2)+6p^2A_0(m_H^2)+3m_H^2A_0(m_W^2)+60p^2A_0(m_W^2)+54p^2A_0(m_Z^2) \\
& +3m_H^4B_0(p^2,m_H^2,m_W^2)-6m_H^2p^2B_0(p^2,m_H^2,m_W^2)+3p^4B_0(p^2,m_H^2,m_W^2)+ \\
& 3m_W^4(B_0(p^2,m_H^2,m_W^2)-B_0(p^2,m_W^2,m_Z^2)) \\
& +3m_W^2m_Z^2B_0(p^2,m_W^2,m_Z^2)-117p^4B_0(p^2,m_W^2,m_Z^2) \\
& +24m_W^4s_W^4(-B_0(p^2,m_\gamma^2,m_W^2)+B_0(p^2,m_W^2,m_Z^2)) \\
& +24m_W^2s_W^4(A_0(m_Z^2)+2(m_\gamma^2+p^2)B_0(p^2,m_\gamma^2,m_W^2)-2p^2B_0(p^2,m_W^2,m_Z^2)) \\
& -12s_W^4\Big[2m_\gamma^2A_0(m_W^2)-4p^2(m_\gamma^2+A_0(m_Z^2)) \\
& +(2m_\gamma^4-7m_\gamma^2p^2-10p^4)B_0(p^2,m_\gamma^2,m_W^2)+10p^4B_0(p^2,m_W^2,m_Z^2]\Big] \\
& +m_W^4s_W^2(24B_0(p^2,m_\gamma^2,m_W^2)-3(B_0(p^2,m_H^2,m_W^2)+B_0(p^2,m_W^2,m_Z^2))) \\
& +s_W^2\Big[-48m_\gamma^2p^2+6m_H^2p^2+4p^4+3(m_H^2-2p^2)A_0(m_H^2) \\
& +3(8m_\gamma^2-m_H^2-20p^2)A_0(m_W^2)+24m_\gamma^4B_0(p^2,m_\gamma^2,m_W^2)-3m_H^4B_0(p^2,m_H^2,m_W^2)- \\
& 3p^2(34A_0(m_Z^2)+4(7m_\gamma^2+10p^2)B_0(p^2,m_\gamma^2,m_W^2)+(-2m_H^2+p^2)B_0(p^2,m_H^2,m_W^2) \\
& -79p^2B_0(p^2,m_W^2,m_Z^2))\Big] \\
& +3m_W^2(A_0(m_H^2)-A_0(m_W^2)-2((m_H^2-5p^2)B_0(p^2,m_H^2,m_W^2) \\
& +p^2(19+30B_0(p^2,m_W^2,m_Z^2)))) \\
& -3m_W^2s_W^2\Big[A_0(m_H^2)-2A_0(m_W^2)+9A_0(m_Z^2)+2(8(m_\gamma^2+p^2)B_0(p^2,m_\gamma^2,m_W^2) \\
& -(m_H^2-5p^2)B_0(p^2,m_H^2,m_W^2)-p^2(18+43B_0(p^2,m_W^2,m_Z^2)))\Big]\Big\} \qquad (143)
\end{aligned}
$$

which after performing the reduction on (142) but before setting $m_\gamma = 0$ in (143) we find an additional term

$$\Pi_{WW}^{\text{Mass Builder}} - \Pi_{WW}^{\text{Ibe}} = \frac{g_2^2 m_\gamma^2 s_W^2 B_0(p^2, m_\gamma^2, m_W^2)}{16\pi^2} \tag{144}$$

which is zero for $m_\gamma = 0$. This is the only difference between our working and that of Ibe et al. [2] where they have clearly set $m_\gamma = 0$.

4.3 One-loop counter-terms

We determine the one-loop counter-term couplings using the inbuilt Mass Builder feature. After all diagrams have been computed, Mass Builder collects all amplitudes together and extracts the coefficient of $1/\epsilon$ and simplifies this to give the one-loop counter term coupling[3]. It also prints out the coefficients of $1/\epsilon^2$ and $1/\epsilon^3$ as a check that higher order divergences do not exist in the one-loop amplitude. With this method we determine the following counter-terms

$$\delta_{Z_{WW}} = -\frac{g_2^2}{16\pi^2}\left(-\frac{11}{6}\right)\Delta, \tag{145}$$

$$\delta_{m^2_{WW}} = -\frac{g_2^2}{16\pi^2}\left(m_Z^2(-1+2s_W^2) - m_\gamma^2 s_W^2\right)\Delta, \tag{146}$$

$$\delta_{Z_{\gamma\gamma}} = -\frac{g_2^2 s_W^2}{16\pi^2}\left(-\frac{5}{3}\right) = \frac{\hat{e}^2}{16\pi^2}\left(-\frac{5}{3}\right)\Delta, \tag{147}$$

$$\delta_{m^2_{\gamma\gamma}} = 0\,, \tag{148}$$

$$\delta_{Z_{ZZ}} = -\frac{g_2^2}{16\pi^2 c_W^2}\left(-\frac{11}{6} + \frac{11}{3}s_W^2 - \frac{5}{3}s_W^4\right)\Delta, \tag{149}$$

$$\delta_{m^2_{ZZ}} = -\frac{g_2^2 m_Z^2}{16\pi^2 c_W^2}\left(-1 + 6s_W^2 - 4s_W^4\right)\Delta, \tag{150}$$

$$\delta_{m^2_{Z\gamma}} = -\frac{g_2^2 s_W}{16\pi^2 c_W}\left(m_Z^2(2-2s_W^2)\right)\Delta, \tag{151}$$

$$\delta_{Z_{Z\gamma}} = -\frac{g_2^2 s_W}{16\pi^2 c_W}\left(\frac{11}{6} - \frac{5s_W^2}{3}\right)\Delta. \tag{152}$$

These match those of Ibe et al. (if we neglect the terms which obviously come from the SM fermionic and leptonic interactions – which our model does not contain) for the case of $m_\gamma = 0$. As there is mixing between the Z boson and the photon we also computed a counter-term coupling for the two point propagator $Z \to \gamma$. This mixing calculation is fully supported in Mass Builder by using the additional −q <particle> option.

[3]This is straightforward as the problem is reduced to a linear algebraic equation, at the two-loop level the problem involves solving a well chosen set of independent simultaneous equations so is currently not supported.

The one-loop counter-term couplings for the fermionic triplet are computed in the same way to give

$$\delta_{Z_{\chi\chi}} = -\frac{g_2^2}{8\pi^2}\Delta, \tag{153}$$

$$\delta_{m_{\chi\chi}} = -\frac{g_2^2 m_\chi}{2\pi^2}\Delta \tag{154}$$

which agree with that of Ibe et al.

4.3.1 Gauge interaction of the triplet

Finally we need the counter-term for the interaction between the triplet and the gauge sector. This is given by Ibe et al. [2] in the following direct quote:

The neutral and charged winos have the $SU(2)_L$ gauge interaction which is described by the term, $\mathcal{L}_{\rm int} = i\epsilon_{abc}(g + \delta_{\tilde{\chi}\tilde{\chi}W})\tilde{\chi}^{a\dagger}\not{W}^b\tilde{\chi}^c$, and the counter-term is given by

$$\delta_{\tilde{\chi}\tilde{\chi}W} = \frac{g^3}{4\pi^2}\Delta\ . \tag{155}$$

The notation that has been used here is not clear. From an understanding of the Lagrangian, we know that there are more interactions than just those between the electroweak triplet (here referred to as a wino) and the W boson, so we must infer that $\not{W}^a = \{W^+, W^-, W^3\}$ where $W^3_\mu = (s_W A_\mu + c_W Z_\mu)$ (see [12] for an example of this notation). This would give us the following renormalised Lagrangian

$$\begin{aligned}
\mathcal{L} =& (g + \delta_{\tilde{\chi}\tilde{\chi}W})\left(\overline{\chi^+}\gamma_\mu {\chi^+}\right)(s_W A_\mu + c_W Z_\mu) \\
&+ (g + \delta_{\tilde{\chi}\tilde{\chi}W})\left(\overline{\chi^+}\gamma_\mu \chi^0\right) W^+_\mu + \text{h.c.} \\
&= g\left(\overline{\chi^+}\gamma_\mu {\chi^+}\right)(s_w A_\mu + c_w Z_\mu) + \left[g\left(\overline{\chi^+}\gamma_\mu \chi^0\right) W^+_\mu + \text{h.c.}\right] \\
&+ s_W\delta_{\tilde{\chi}\tilde{\chi}W}\left(\overline{\chi^+}\gamma_\mu {\chi^+}\right) A_\mu + c_W\delta_{\tilde{\chi}\tilde{\chi}W}\left(\overline{\chi^+}\gamma_\mu {\chi^+}\right) Z_\mu \\
&+ \left[\delta_{\tilde{\chi}\tilde{\chi}W}\left(\overline{\chi^+}\gamma_\mu \chi^0\right) W^+_\mu + \text{h.c.}\right]
\end{aligned} \tag{156}$$

so the resultant counter-terms we need to add into the calculation are $\delta_{\tilde{\chi}\tilde{\chi}W}$, $s_W\,\delta_{\tilde{\chi}\tilde{\chi}W}$ and $c_W\,\delta_{\tilde{\chi}\tilde{\chi}W}$ for the $W\chi\chi^\dagger$, $A\chi\chi$ and $Z\chi\chi$ vertices respectively.

4.4 Two-loop self energy

We are finally ready to compute the two-loop self energy for the electroweak triplet. For the neutral (charged) component there are 48 (75) two-loop diagrams and eight (10) counter-term diagrams of two-loop order.

To compute the pole mass correctly, and thus the mass splitting, we also need to evaluate the derivatives of the one-loop self energies. This is not required if we are to compute the pole mass via the iterative method, but we will leave that until a later section. The derivates of the one loop self energies were computed by hand and are provided with Mass Builder in the supplements namespace defined in the file src/supplements.cpp. The triplet cmake target creates an executable that will retrieve both the two-loop amplitudes and the derivatives of the one-loop self energies to produce the full two-loop mass splitting.

Figures 4, 5, 6 and 7 give the diagrams of two-loop order.

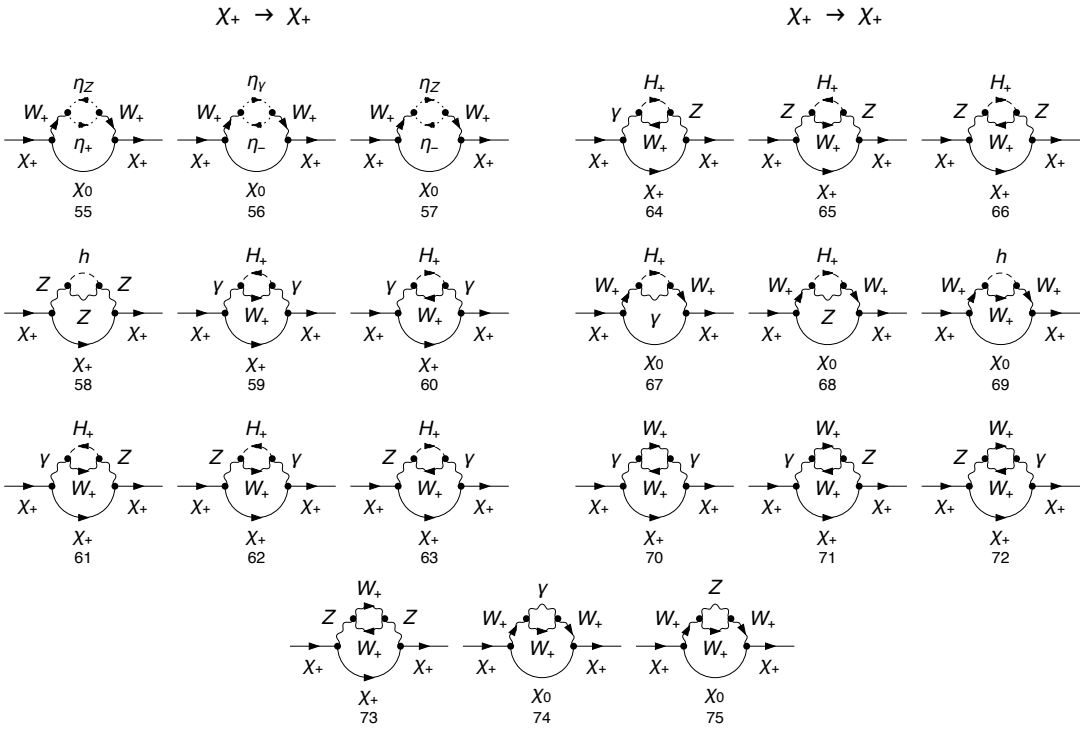

Figure 4: The two-loop corrections to the χ^+ propagator.

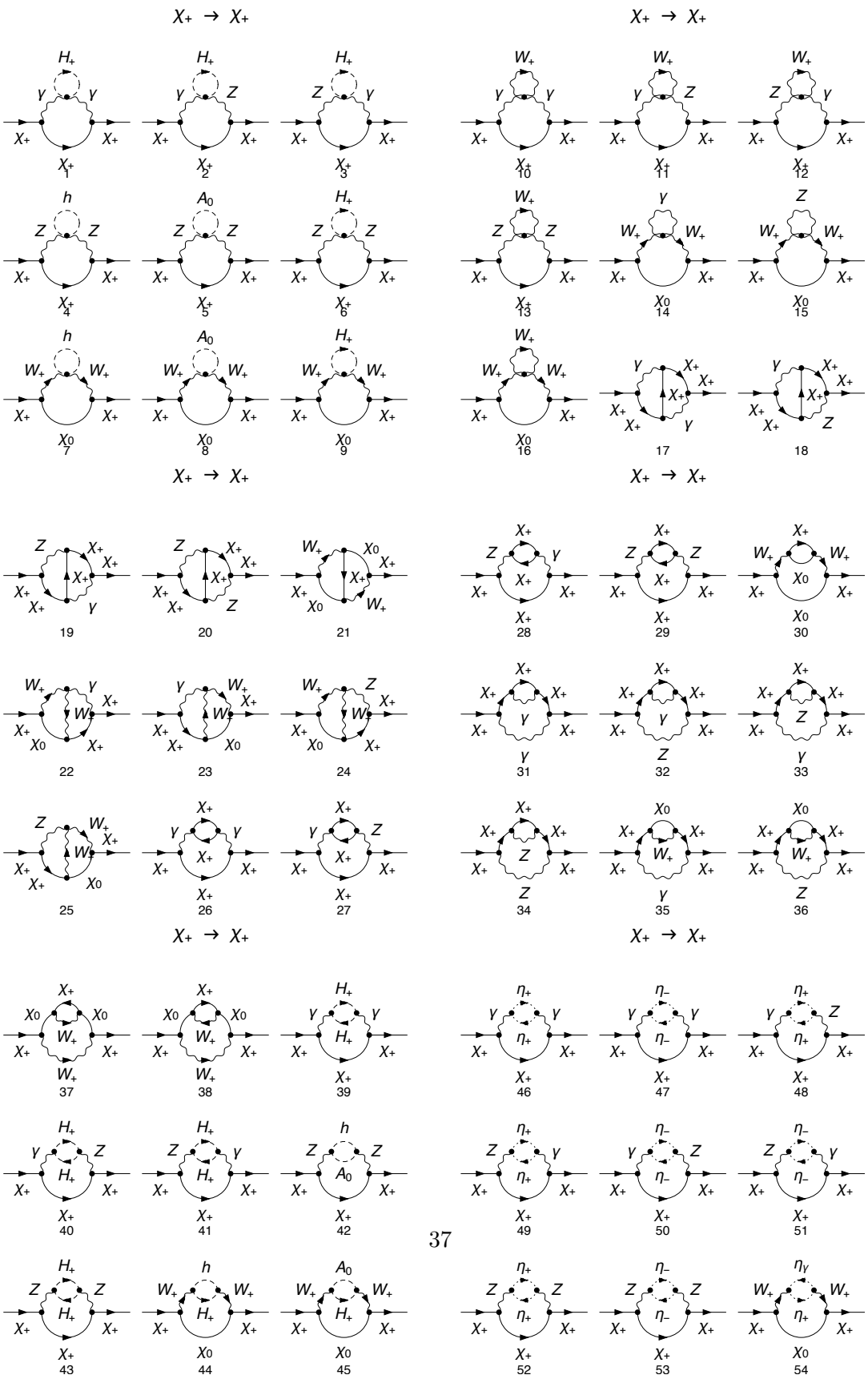

Figure 5: The two-loop corrections to the χ^+ propagator.

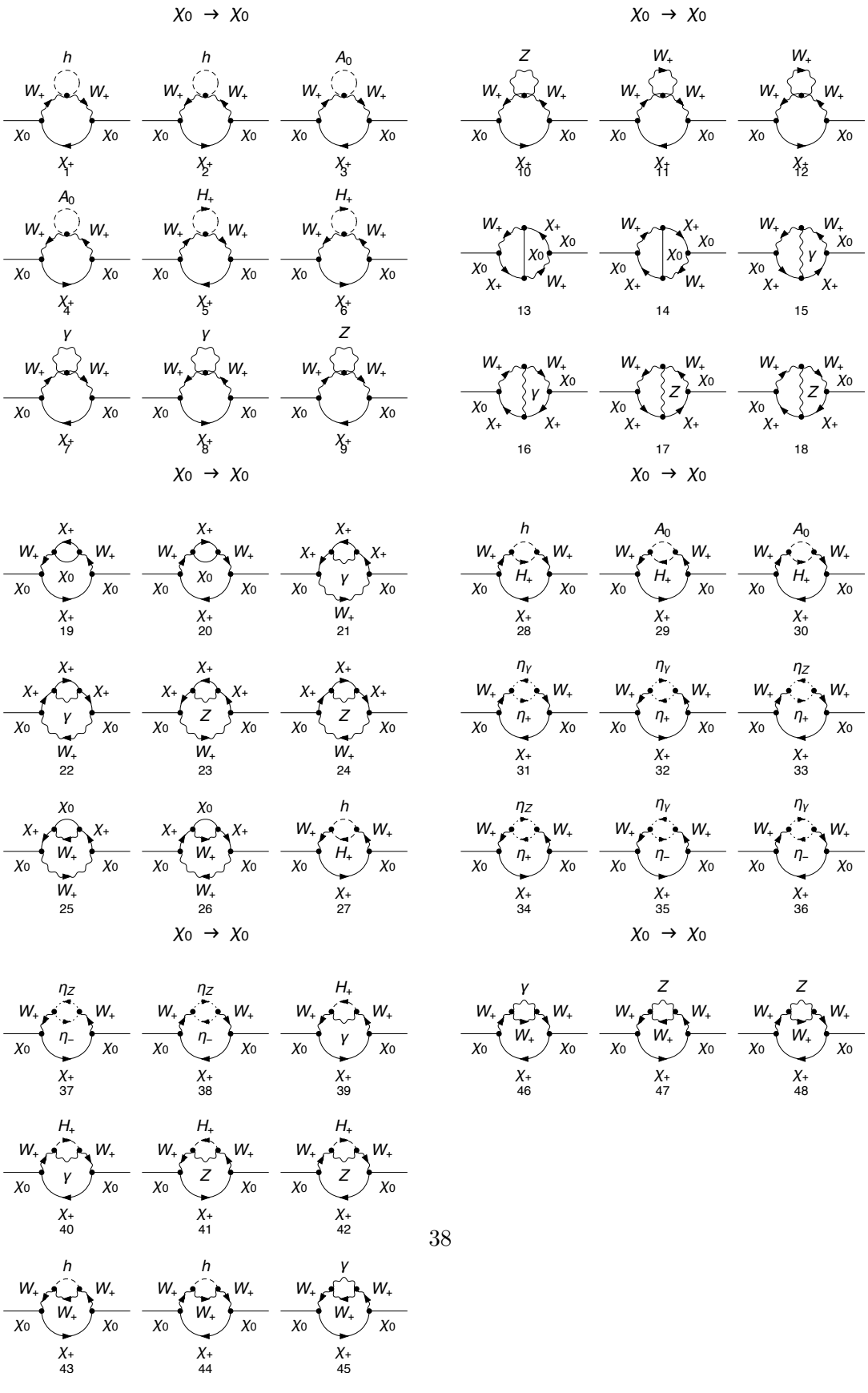

Figure 6: The two-loop corrections to the χ^0 propagator.

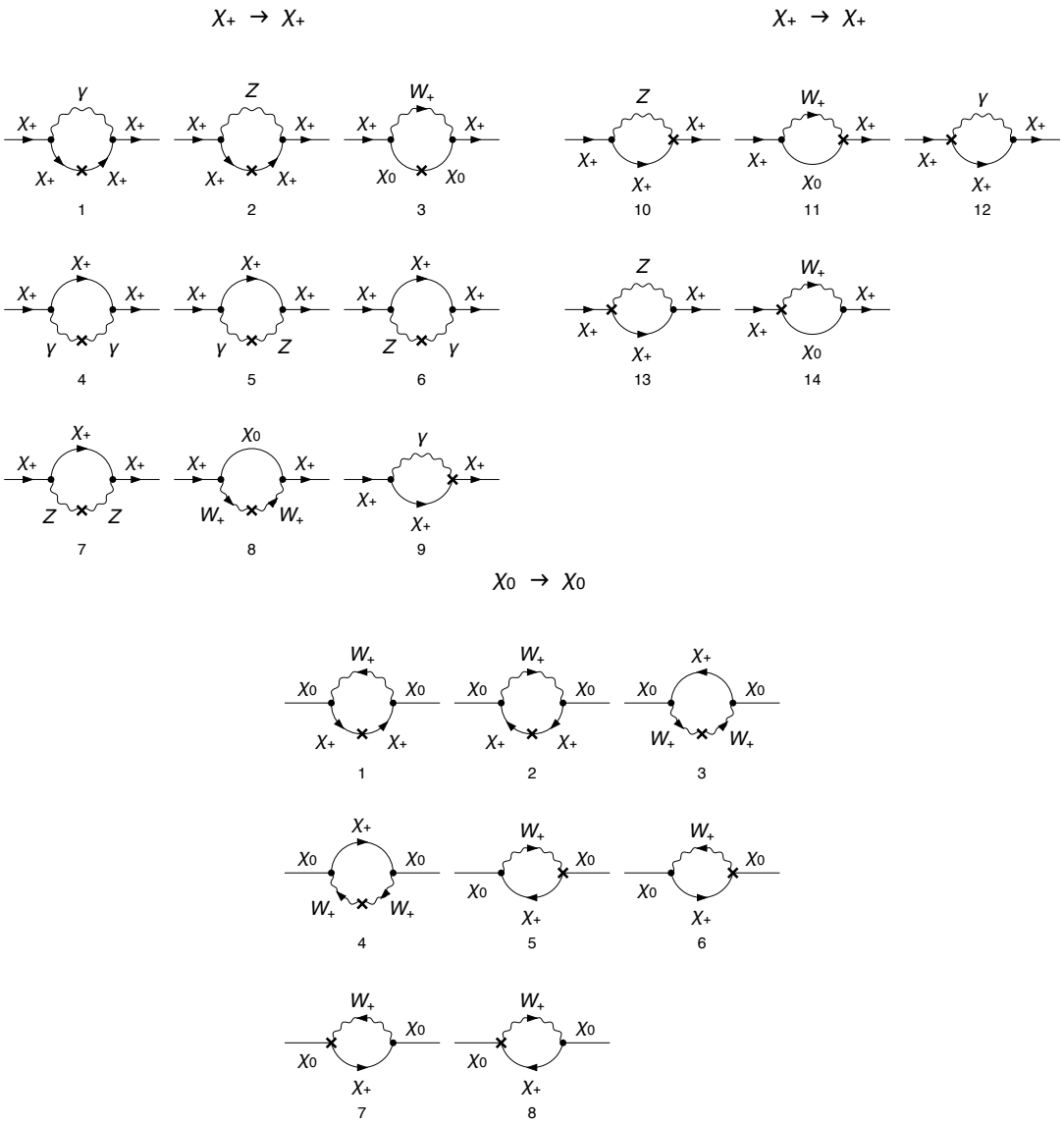

Figure 7: The two-loop order counter-terms corrections to the χ^+ and χ^0 propagators.

4.4.1 Cancellation of diagrams

Referring again to this Wikipedia article which cites an old book we have the following direct quote:

In Feynman diagrams the ghosts appear as closed loops wholly composed of 3-vertices, attached to the rest of the diagram via a gauge particle at each 3-vertex. Their contribution to the S-matrix is exactly cancelled (in the Feynman-'t Hooft gauge) by a contribution from a similar loop of gauge particles with only 3-vertex couplings or gauge attachments to the rest of the diagram.[4] (A loop of gauge particles not wholly composed of 3-vertex couplings is not cancelled by ghosts.) The opposite sign of the contribution of the ghost and gauge loops is due to them having opposite fermionic/bosonic natures. (Closed fermion loops have an extra -1 associated with them; bosonic loops don't.)

4.4.2 IR divergences

From this paper on page 5, right hand side, it mentions the divergent integral I find in some of the amplitudes (see the Mathematica script show_sum_still_IR_divergent) and says that these should always cancel from physical quantities. Check that this occurs, look for both the T and V integrals involved here.

We expect there to be IR divergences arising from a specific set of diagrams, as described by Ibe et al. in the following direct quote [2]:

For the charged wino, the amplitude in [ref. [2] – Figure 2(i)] in which a photon is circulating in the outer loop and the one in [the counter-term diagram] [ref. [2] – Figure 3(b)] with the photon loop behave as

$$\Sigma^{(2)}_{K,M}(p^2 = \hat{M}_2^2) \sim \int \frac{d^4k}{(2\pi)^4} \frac{1}{(k\cdot p)^2} \frac{1}{k^2} \ , \tag{157}$$

and hence, they are IR divergent. In addition, the derivatives, $\dot{\Sigma}^{(1)}_{K,M}|_{p^2=\hat{M}_2^2}$, are also IR divergent due to the diagram including a photon propagator.

In our approach we wish to set a finite mass for the photon, as this still gives the same phenomenology for the mass splittings at the one-loop level. Therefore any interesting effects at the two-loop level should be able to be studied with a small but finite photon mass. The cancellation between IR divergences mentioned above should also occur numerically if we set a small photon mass, resulting in a still reasonable total amplitude.

However, we find that there are significantly more diagrams which are ill-defined in the limit of $m_\gamma \to 0$ than suggested by Ibe et al. [2]. We have two options when computing these. First, we can either set $m_\gamma = 0$ from the outset, then we will end up with an amplitude proportional to $(p^2 - m_\chi^2)^{-1}$, which is ill-defined for the important case of $p^2 = m_\chi^2$ (either in the implicit or explicit calculation of the pole mass, the amplitudes must be finite here). The second option is to leave a finite m_γ throughout the calculation and subsequent basis integral reduction, and substitute $m_\gamma \to 0$ at the end. This results in an amplitude proportional to m_γ^{-2} or in a basis integral which is not defined at $m_\gamma = 0$, so again this is ill-defined.

One possibility is that our diagram by diagram approach is flawed because of missing cancellations between diagrams. To investigate this we compute the diagrams with a finite m_γ throughout and then attempt to evaluate the result with $m_\gamma = 0$. The IR divergence is not always evident from a m_γ^{-2} factor as it may be that one of the basis integrals is ill-defined, so we check that a diagram is finite by numerical evaluation. We then compose a list of diagrams which are undefined (in this case all returning an inf result) and sum these together. If there is any important cancellation that would solve the problem, it would occur between these ill-defined diagrams, and not from any other finite diagram. So we only have a handful of amplitudes to sum together, which is an achievable yet still cumbersome task for an analytical simplifier. We find that the resultant sum still contains integrals which are ill-defined at $m_\gamma = 0$, such as $T(m_\gamma, m_\chi, m_W)$.

So we find that for the neutral component of the triplet, every diagram which includes a photon propagator, in any leg, is IR divergent, and the sum of these is also IR divergent.

4.4.3 Numerical results

The most powerful feature of Mass Builder is the automatic generation of an interface to TSIL. This provides a fast and reliable method of obtaining a numerical result for the self energies at one and two-loop order. The only alternative would be a semi-automatic process at best, with the possibility of missing a contribution or making a minor error being left to chance.

The input parameters and resultant self energies and pole masses are given in Table 3.

Table 3: The parameter values used for the electroweak triplet self energy calculations. Where a derived quantity is used this is passed directly to Mass Builder in the analytic form.

Parameter	Value
m_W	80.385 GeV
m_Z	91.1876 GeV
m_H	125.6 GeV
m_χ	100 GeV
m_γ	–
v	246 GeV
Q	100 GeV
c_W^2	m_W^2/m_Z^2
s_W^2	$1 - c_W^2$
g_2	$2m_W/v$
g_1	$g_2 s_W/c_W$

Table 4: The total self energies for $p = m_\chi = 5 \times 10^3$ GeV, $m_\gamma = 0$ (*left*), $m_\gamma = 10$ GeV (*right*), and the remaining parameters as given in Table 3.

Field	1-loop self energy (GeV)
W	–
Z	–
γ	–
χ^+	–
χ^0	–

Field	1-loop self energy (GeV)
W	–
Z	–
γ	–
χ^+	–
χ^0	–

Field	2-loop self energy (GeV)
χ^+	–
χ^0	–

Field	2-loop self energy (GeV)
χ^+	–
χ^0	–

Field	Physical mass (GeV)
W	–
Z	–
γ	–

Field	Physical mass (GeV)
W	–
Z	–
γ	–

Table 5: The finite amplitudes of each one-loop diagram for $p = m_\chi = 5 \times 10^3$ GeV, $m_\gamma = 0$ (*left*), $m_\gamma = 10$ GeV (*right*), and the remaining parameters as given in Table 3.

Particle	Diagram	Amplitude (GeV)	Particle	Diagram	Amplitude (GeV)
χ^+	1	100.379	χ^+	1	100.379
χ^+	2	351.02	χ^+	2	351.02
χ^+	3	451.522	χ^+	3	451.522
χ^0	1	451.522	χ^0	1	451.522
χ^0	2	451.522	χ^0	2	451.522

Table 6: The finite amplitudes of each two-loop diagram for $p = m_\chi = 5\times10^3$ GeV, $m_\gamma = 0$ (*left*), $m_\gamma = 10$ GeV (*right*), and the remaining parameters as given in Table 3.

Particle	Diagram	Amplitude (GeV)	Particle	Diagram	Amplitude (GeV)
χ^+	1	0.733985	χ^+	1	–
χ^+	2	0.409273	χ^+	2	0.40449
χ^+	3	0.409273	χ^+	3	0.40449
χ^+	4	1.16585	χ^+	4	1.16585
χ^+	5	0.614187	χ^+	5	0.614187
χ^+	6	0.293129	χ^+	6	0.293129
χ^+	7	1.49846	χ^+	7	1.49846
χ^+	8	0.789463	χ^+	8	0.789463
χ^+	9	1.22676	χ^+	9	1.22676
χ^+	10	-0.222797	χ^+	10	–
χ^+	11	3.57161	χ^+	11	3.53008
χ^+	12	3.57161	χ^+	12	3.53008
χ^+	13	6.91987	χ^+	13	6.91987
χ^+	14	0.0253242	χ^+	14	0
χ^+	15	7.36556	χ^+	15	7.36556
χ^+	16	7.36419	χ^+	16	7.36419
χ^+	17	-0.838939	χ^+	17	-0.837416
χ^+	18	-2.36083	χ^+	18	-2.35887
χ^+	19	-2.36083	χ^+	19	-2.35887
χ^+	20	-16.3858	χ^+	20	-16.3858
χ^+	21	-27.1077	χ^+	21	-27.1077
χ^+	22	-11.3453	χ^+	22	–
χ^+	23	-11.3453	χ^+	23	–
χ^+	24	-50.1025	χ^+	24	-50.1025
χ^+	25	-50.1025	χ^+	25	-50.1025
χ^+	26	28501.9	χ^+	26	–
χ^+	27	-6248.66	χ^+	27	–
χ^+	28	-6248.66	χ^+	28	–
χ^+	29	10.1439	χ^+	29	10.1439
χ^+	30	16.7793	χ^+	30	16.7793
χ^+	31	-2.82652	χ^+	31	–
χ^+	32	-10.7346	χ^+	32	–
χ^+	33	-9.74724	χ^+	33	–
χ^+	34	-37.4303	χ^+	34	-37.4303
χ^+	35	-12.5502	χ^+	35	–

Table 7: *Continued from Table 6 ...* The finite amplitudes of each two-loop diagram for $p = m_\chi = 5 \times 10^3$ GeV, $m_\gamma = 0$ (*left*), $m_\gamma = 10$ GeV (*right*), and the remaining parameters as given in Table 3.

Particle	Diagram	Amplitude (GeV)	Particle	Diagram	Amplitude (GeV)
χ^+	36	-48.1651	χ^+	36	-48.1651
χ^+	37	-62.6267	χ^+	37	-62.6267
χ^+	38	-62.6267	χ^+	38	-62.6267
χ^+	39	-1.6302	χ^+	39	–
χ^+	40	0.0653375	χ^+	40	–
χ^+	41	0.0653375	χ^+	41	–
χ^+	42	-0.76785	χ^+	42	-0.76785
χ^+	43	0.0179657	χ^+	43	0.0179657
χ^+	44	-1.10023	χ^+	44	-1.10023
χ^+	45	-0.390827	χ^+	45	-0.390827
χ^+	46	0.407549	χ^+	46	–
χ^+	47	0.407549	χ^+	47	–
χ^+	48	-0.0458078	χ^+	48	–
χ^+	49	-0.0458078	χ^+	49	–
χ^+	50	-0.0458078	χ^+	50	–
χ^+	51	-0.0458078	χ^+	51	–
χ^+	52	-0.0353232	χ^+	52	-0.0353232
χ^+	53	-0.0353232	χ^+	53	-0.0353232
χ^+	54	-0.0869555	χ^+	54	–
χ^+	55	0.303712	χ^+	55	0.303712
χ^+	56	-0.0869555	χ^+	56	–
χ^+	57	0.303712	χ^+	57	0.303712
χ^+	58	2.46149	χ^+	58	2.46149
χ^+	59	0.712412	χ^+	59	–
χ^+	60	0.712412	χ^+	60	–
χ^+	61	-0.00132902	χ^+	61	-0.0013774
χ^+	62	-0.00132902	χ^+	62	-0.0013774
χ^+	63	-0.00132902	χ^+	63	-0.0013774
χ^+	64	-0.00132902	χ^+	64	-0.0013774
χ^+	65	0.0950094	χ^+	65	0.0950094
χ^+	66	0.0950094	χ^+	66	0.0950094
χ^+	67	0.547568	χ^+	67	–
χ^+	68	0.157117	χ^+	68	0.157117
χ^+	69	2.4579	χ^+	69	2.4579
χ^+	70	-6.51295	χ^+	70	–

Table 8: *Continued from Table 7 ...* The finite amplitudes of each two-loop diagram for $p = m_\chi = 5 \times 10^3$ GeV, $m_\gamma = 0$ (*left*), $m_\gamma = 10$ GeV (*right*), and the remaining parameters as given in Table 3.

Particle	Diagram	Amplitude (GeV)	Particle	Diagram	Amplitude (GeV)
χ^+	71	-7.84551	χ^+	71	–
χ^+	72	-7.84551	χ^+	72	–
χ^+	73	-35.0007	χ^+	73	-35.0007
χ^+	74	-11.5835	χ^+	74	–
χ^+	75	-51.2921	χ^+	75	-51.2921
χ^0	1	1.49846	χ^0	1	1.49846
χ^0	2	1.49846	χ^0	2	1.49846
χ^0	3	0.789463	χ^0	3	0.789463
χ^0	4	0.789463	χ^0	4	0.789463
χ^0	5	1.22676	χ^0	5	1.22676
χ^0	6	1.22676	χ^0	6	1.22676
χ^0	7	0.0253242	χ^0	7	0
χ^0	8	0.0253242	χ^0	8	0
χ^0	9	7.36556	χ^0	9	7.36556
χ^0	10	7.36556	χ^0	10	7.36556
χ^0	11	7.36419	χ^0	11	7.36419
χ^0	12	7.36419	χ^0	12	7.36419
χ^0	13	-27.1077	χ^0	13	-27.1077
χ^0	14	-27.1077	χ^0	14	-27.1077
χ^0	15	-14.3658	χ^0	15	–
χ^0	16	-14.3658	χ^0	16	–
χ^0	17	-50.0832	χ^0	17	-50.0832
χ^0	18	-50.0832	χ^0	18	-50.0832
χ^0	19	16.7793	χ^0	19	16.7793
χ^0	20	16.7793	χ^0	20	16.7793
χ^0	21	-13.9575	χ^0	21	–
χ^0	22	-13.9575	χ^0	22	–
χ^0	23	-48.6688	χ^0	23	-48.6688
χ^0	24	-48.6688	χ^0	24	-48.6688
χ^0	25	-62.6267	χ^0	25	-62.6267
χ^0	26	-62.6267	χ^0	26	-62.6267
χ^0	27	-1.10023	χ^0	27	-1.10023
χ^0	28	-1.10023	χ^0	28	-1.10023
χ^0	29	-0.390827	χ^0	29	-0.390827
χ^0	30	-0.390827	χ^0	30	-0.390827

Table 9: *Continued from Table 8 ...* The finite amplitudes of each two-loop diagram for $p = m_\chi = 5 \times 10^3$ GeV, $m_\gamma = 0$ (*left*), $m_\gamma = 10$ GeV (*right*), and the remaining parameters as given in Table 3.

Particle	Diagram	Amplitude (GeV)	Particle	Diagram	Amplitude (GeV)
χ^0	31	-0.0869555	χ^0	31	–
χ^0	32	-0.0869555	χ^0	32	–
χ^0	33	0.303712	χ^0	33	0.303712
χ^0	34	0.303712	χ^0	34	0.303712
χ^0	35	-0.0869555	χ^0	35	–
χ^0	36	-0.0869555	χ^0	36	–
χ^0	37	0.303712	χ^0	37	0.303712
χ^0	38	0.303712	χ^0	38	0.303712
χ^0	39	0.547568	χ^0	39	–
χ^0	40	0.547568	χ^0	40	–
χ^0	41	0.157117	χ^0	41	0.157117
χ^0	42	0.157117	χ^0	42	0.157117
χ^0	43	2.4579	χ^0	43	2.4579
χ^0	44	2.4579	χ^0	44	2.4579
χ^0	45	-11.5835	χ^0	45	–
χ^0	46	-11.5835	χ^0	46	–
χ^0	47	-51.2921	χ^0	47	-51.2921
χ^0	48	-51.2921	χ^0	48	-51.2921

Table 10: The finite amplitudes of each two-loop counter-term diagram for $p = m_\chi = 5\times10^3$ GeV, $m_\gamma = 0$ (*left*), $m_\gamma = 10$ GeV (*right*), and the remaining parameters as given in Table 3.

Particle	Diagram	Amplitude (GeV)	Particle	Diagram	Amplitude (GeV)
χ^+	1	22.7298	χ^+	1	–
χ^+	2	76.9668	χ^+	2	76.9668
χ^+	3	99.1773	χ^+	3	99.1773
χ^+	4	0.582979	χ^+	4	–
χ^+	5	-1.49941	χ^+	5	-1.49951
χ^+	6	-1.49941	χ^+	6	-1.49951
χ^+	7	8.10658	χ^+	7	8.10658
χ^+	8	11.1957	χ^+	8	11.2042
χ^+	9	-18.4632	χ^+	9	-18.4632
χ^+	10	-18.4632	χ^+	10	-18.4632
χ^+	11	-18.4632	χ^+	11	-18.4632
χ^+	12	-4.1037	χ^+	12	-4.10396
χ^+	13	-14.3563	χ^+	13	-14.3563
χ^+	14	-18.4632	χ^+	14	-18.4632
χ^0	1	99.1773	χ^0	1	99.1773
χ^0	2	99.1773	χ^0	2	99.1773
χ^0	3	11.1957	χ^0	3	11.2042
χ^0	4	11.1957	χ^0	4	11.2042
χ^0	5	-18.4632	χ^0	5	-18.4632
χ^0	6	-18.4632	χ^0	6	-18.4632
χ^0	7	-18.4632	χ^0	7	-18.4632
χ^0	8	-18.4632	χ^0	8	-18.4632

A Definitions

We will make use of tools and literature sources which use slightly different definitions for the same mathematical objects. In this section we make it clear what these differences are and how these differences alter the important relationships between these objects.

In the following I use bold-face for the divergent integrals and normal type for the finite pieces, as defined in the TSIL manual [1]. I use `TAI` to refer to TARCER notation and A for TSIL notation as there is a different normalisation between such integrals. We define $\kappa = 1/16\pi^2$.
We begin with B_0 and B_1. These are defined by Ibe at al. [2] as

$$B_0(p^2, m_1^2, m_2^2) = \Delta - \int_0^1 dx \ \log \frac{(1-x)m_1^2 + xm_2^2 - x(1-x)p^2 - i\epsilon}{Q^2} , \quad (158)$$

$$B_1(p^2, m_1^2, m_2^2) = -\frac{\Delta}{2} + \int_0^1 dx \ x \log \frac{(1-x)m_1^2 + xm_2^2 - x(1-x)p^2 - i\epsilon}{Q^2} , \quad (159)$$

$$B_{21}(p^2, m_1^2, m_2^2) = \frac{\Delta}{3} - \int_0^1 dx \ x^2 \log \frac{(1-x)m_1^2 + xm_2^2 - x(1-x)p^2 - i\epsilon}{Q^2} , \quad (160)$$

while Pierce, Bagger, Matchev and Zhang [13] (henceforth BMPZ) defines these as

$$A_0(m) = 16\pi^2 Q^{4-n} \int \frac{d^n q}{i\,(2\pi)^n} \frac{1}{q^2 - m^2 + i\varepsilon} \quad (161)$$

$$B_0(p, m_1, m_2) = 16\pi^2 Q^{4-n} \int \frac{d^n q}{i\,(2\pi)^n} \frac{1}{\left[q^2 - m_1^2 + i\varepsilon\right]\left[(q-p)^2 - m_2^2 + i\varepsilon\right]} \quad (162)$$

$$p_\mu B_1(p, m_1, m_2) = 16\pi^2 Q^{4-n} \int \frac{d^n q}{i\,(2\pi)^n} \frac{q_\mu}{\left[q^2 - m_1^2 + i\varepsilon\right]\left[(q-p)^2 - m_2^2 + i\varepsilon\right]} \quad (163)$$

$$p_\mu p_\nu B_{21}(p, m_1, m_2) + g_{\mu\nu} B_{22}(p, m_1, m_2) \quad (164)$$
$$= 16\pi^2\, Q^{4-n} \int \frac{d^n q}{i\,(2\pi)^n} \frac{q_\mu q_\nu}{\left[q^2 - m_1^2 + i\varepsilon\right]\left[(q-p)^2 - m_2^2 + i\varepsilon\right]} ,$$

where we deal with B_{22} later.

The above definitions are not equivalent, first we need to set $\Delta = 2/(4-D) - \gamma_E + \log(4\pi)$ and $n = D$. However, there is an important sign difference from the way the denominator is written. BMPZ use $(p-k)$ while other sources, including Ibe et al. use $(p+k)$. Therefore when doing the Feynman integration and introducing the step, we end up shifting the integration measure, k, by either $k + px$ or $k - px$. This difference introduces a sign

difference in the integrated form of B_1. (need to check the validity of the relationship given in B.9 in BMPZ for the case of $(k+p)$. Therefore when we compare with the results stated in Ibe et al. we must be careful with the sign of the B_1 integral and make sure to introduce a negative. TSIL defines

$$\mathbf{A}(x) = C\int d^dk \frac{1}{[k^2+x]} \tag{165}$$

$$\mathbf{B}(x,y) = C\int d^dk \frac{1}{[k^2+x][(k-p)^2+y]}. \tag{166}$$

where

$$C = (16\pi^2)\frac{\mu^{2\epsilon}}{(2\pi)^d} = (2\pi\mu)^{2\epsilon}/\pi^2. \tag{167}$$

and TARCER uses

$$\mathbf{A}(x) = ia\texttt{TAI[d,s,}\{\{1,\sqrt{x}\}\}], \tag{168}$$

$$\mathbf{B}(x,y) = -ia\texttt{TBI[d,s,}\{\{1,\sqrt{x}\},\{1,\sqrt{y}\}\}] \tag{169}$$

where $a = (4\pi\mu^2)^{2-d/2}$. So we make the identification that $d = 4-2\epsilon$ and achieve equivalent pre-factors. There is an important sign difference attached to the $m^2 = x$ quantity between the different definitions of A_0 and B_0. The effects the form of the finite plus divergent expansion of the basis integrals. From the TSIL manual we have

$$\mathbf{A}(x) = -x/\epsilon + A(x) + \epsilon A_\epsilon(x) + \mathcal{O}(\epsilon^2) \tag{170}$$

$$\mathbf{B}(x,y) = 1/\epsilon + B(x,y) + \epsilon B_\epsilon(x,y) + \mathcal{O}(\epsilon^2), \tag{171}$$

so to make use of these with TARCER functions we must make the conversion to the form

$$\mathbf{A}(x) = -x/\epsilon + A(x) + \epsilon A_\epsilon(x) + \mathcal{O}(\epsilon^2) \tag{172}$$

$$\mathbf{B}(x,y) = 1/\epsilon + B(x,y) + \epsilon B_\epsilon(x,y) + \mathcal{O}(\epsilon^2), \tag{173}$$

So Ibe et al. do not define an A_0 function, instead using only B_1 which we can reduce down to a function of B_0 and A_0. This relationship is essential for our calculations, and we will present it shortly. First we need to draw a direct comparison between the above function definitions.

B Tensor integral reduction

We need to compare self energies calculated with Mass Builder and those in the existing literature. Comparing with Ibe et al. we need to understand the definitions used.

Ibe et al. make the following definitions:

$$\Pi_V = -p^2 \left[B_1(p^2, m_1^2, m_2^2) + B_{21}(p^2, m_1^2, m_2^2) \right] \tag{174}$$

$$\tilde{B}_{22}(p^2, m_1^2, m_2^2) = -p^2(B_1 + B_{21}) - \frac{p^2}{4} B_0 - \frac{1}{4}(m_1^2 - m_2^2)(B_0 + 2B_1) \tag{175}$$

so to compare with the self energies presented within we need to determine exactly what B_{21} is. This requires finding equivalent definitions elsewhere to properly understand what is going on here.
In general we find the statement

$$\begin{aligned} B_{\mu\nu} &= g_{\mu\nu} B_{00} + p_\mu p_\nu B_{11} \\ &= g_{\mu\nu} B_{22} + p_\mu p_\nu B_{21} \end{aligned} \tag{176}$$

using FeynCalc to reduce the following (note that in FeynCalc notation B_{22} is denoted B_{00})

```
In[2]:= B22 = PaVe[0, 0, {p^2}, {m1^2,m2^2}]
        B22r = PaVeReduce[B22]

Out[2]= A0[m2^2]/(2 (-1 + D)) + (m1^2 B0[p^2, m1^2, m2^2])/(-1 + D) + (
         m1^2 B1[p^2, m1^2, m2^2])/(2 (-1 + D)) - (m2^2 B1[p^2, m1^2, m2^2])/(
         2 (-1 + D)) + (p^2 B1[p^2, m1^2, m2^2])/(2 (-1 + D))
```

next we need to further reduce the B_1 functions using

```
In[3]:= B22r =
        B22r/.B1-> -(-A0[m1^2]+A0[m2^2]+(p^2+m1^2-m2^2)*B0))/(2 p^2)
```

we then to extract the finite pieces of this integral so we may compare with other sources.

```
In[4]:= CAw1 = Coefficient[B22r, A0[m1^2]] /. D-> 4-2\[Epsilon]
        CAw2 = Coefficient[B22r, A0[m2^2]] /. D-> 4-2\[Epsilon]
        CBww = Coefficient[B22r, B0[p^2,m1^2,m2^2]] /. D-> 4-2\[Epsilon]
        A1 = A0[m1^2] + (m1^2/\[Epsilon]);
        A2 = A0[m1^2] + (m2^2/\[Epsilon]);
        Bww = B0[p^2,m1^2,m2^2] + (1/\[Epsilon]);
        B22finite =
         Coefficient[CAw1*Aw1+CAw2*Aw2+CBww*Bww, \[Epsilon], 0]
```

we first want to check that this is consistent with the definition given in BMPZ [13], which is

$$
\begin{aligned}
B_{22}(p,m_1,m_2) &= \frac{1}{6}\left\{\frac{1}{2}\Big(A_0(m_1)+A_0(m_2)\Big)+\Big(m_1^2+m_2^2-\frac{1}{2}p^2\Big)B_0(p,m_1,m_2)\right. \\
&+ \frac{m_2^2-m_1^2}{2p^2}\Big[A_0(m_2)-A_0(m_1)-(m_2^2-m_1^2)B_0(p,m_1,m_2)\Big] \\
&+ \left. m_1^2+m_2^2-\frac{1}{3}p^2\right\}. \qquad (177)
\end{aligned}
$$

and we find that these expressions do indeed agree. This confirms that the FeynCalc definition of B_{00} does indeed agree with the alternative used in the literature which is B_{22}.

We now need to determine exactly what the notation used in Ibe et al. is. From BMPZ we have

$$\tilde{B}_{22}(p,m_1,m_2) = B_{22}(p,m_1,m_2) - \frac{1}{4}A_0(m_1) - \frac{1}{4}A_0(m_2) \qquad (178)$$

and from Ibe et al. we have

$$\tilde{B}_{22}(p^2,m_1^2,m_2^2) = -p^2(B_1+B_{21}) - \frac{p^2}{4}B_0 - \frac{1}{4}(m_1^2-m_2^2)(B_0+2B_1)\ . \qquad (179)$$

so we have one undefined term here, B_{21}. This is given in Ibe et al. in it's integrated form but we want it in terms of reduced one-loop basis integrals. So, to determine this we will make the assumption that (178) and (179) are equivalent and determine an ansatz for B_{21}. We will then confirm this ansatz by calculating equation (B.5) from Ibe et al. independently and determining what B_{21} is. Comparing equations (178) and (179) we determine

$$B_{21}(p^2,m_1^2,m_2^2) = \frac{1}{18p^2}\Big(6(p^2-m_1^2)B_0(p^2,m_1^2,m_2^2)+6A_0(m_1^2)-6m_1^2+p^2\Big) \qquad (180)$$

Now we calculate the contribution of the electroweak triplet state to the W boson self energy to double check if this definition of B_{21} is consistent. Calculating the required amplitude using Mass Builder we find

$$\Pi_{WW}^{(\tilde{\chi})}(p^2) = \frac{g^2}{36\pi^2}\Big(3(2M^2+p^2)B_0(p^2,M^2,M^2)-6A_0(M^2)+6M^2-p^2\Big) \qquad (181)$$

which is consistent with the Ibe at al. calculation

$$
\begin{aligned}
\Pi_{WW}^{(\tilde{\chi})}(p^2) =& \frac{g^2}{2\pi^2}\Pi_V(p^2,\hat{M}_2^2,\hat{M}_2^2) && (182)\\
=& \frac{g^2}{2\pi^2}\Big\{-p^2\Big[B_1(p^2,m_1^2,m_2^2)+B_{21}(p^2,m_1^2,m_2^2)\Big]\Big\} && (183)
\end{aligned}
$$

which after using $B_1 = -B_0/2$ (since $m_1 = m_2$) we obtain a consistent result.

C Electroweak triplet SARAH model

We use SARAH [11] to generate the FeynArts model file for the electroweak triplet model. The SARAH input model file is presented below.

This is generated using the following commands

```
In[5]:= Import["/Users/jamesmckay/Documents/Programs/SARAH-4.7.0/SARAH.m"]
        Start["EW_triplet"]
        ModelOutput[EWSB, WriteFeynArts -> True,WriteTex->True];

In[6]:= Off[General::spell]
        Model`Name = "EW_triplet";
        Model`NameLaTeX ="EW_triplet";
        Model`Authors = "J. McKay";
        Model`Date = "2016-01";

        (* Gauge Groups *)

        Gauge[[1]]={B,   U[1], hypercharge, g1,False};
        Gauge[[2]]={WB, SU[2], left,        g2,True};

        (* Matter Fields *)

        FermionFields[[1]] = {r, 1,
        { { nL /Sqrt[2], cL } , { conj[cR] , -nL/Sqrt[2] } }
        ,0, 3};

        ScalarFields[[1]] =  {H, 1, {Hp, H0},     1/2, 2};

        (*   DEFINITION   *)

        NameOfStates={GaugeES, EWSB};

        (* ----- Before EWSB ----- *)

        DEFINITION[GaugeES][LagrangianInput]= {
                {LagHC, {AddHC->True}},
                {LagNoHC,{AddHC->False}}
        };
        LagNoHC = mu2 conj[H].H - \[Lambda] conj[H].H.conj[H].H;
        LagHC =  -Yc/2 r.r;
```

```
(* Gauge Sector *)

DEFINITION[EWSB][GaugeSector] =
{
  {{VB,VWB[3]},{VP,VZ},ZZ},
  {{VWB[1],VWB[2]},{VWp,conj[VWp]},ZW}
};

(* ----- VEVs ---- *)

DEFINITION[EWSB][VEVs]=
{{H0, {v, 1/Sqrt[2]}, {Ah, \[ImaginaryI]/Sqrt[2]},{hh, 1/Sqrt[2]}}};

(* Dirac-Spinors *)

DEFINITION[EWSB][Phases] = {
    {Fc, PhaseFc},
    {Fn, PhaseFn}
};
DEFINITION[EWSB][DiracSpinors]={
  Fc ->{  cL, cR},
  Fn ->{  nL,conj[nL]}};
DEFINITION[EWSB][GaugeES]={
 Fc1 ->{ FcL, 0 },
 Fc2 ->{ 0,  FcR}}
```

References

[1] S. P. Martin, D. G. Robertson, *Computer Physics Communications* **174**(2), 133 (2006).

[2] M. Ibe, S. Matsumoto, R. Sato, *Physics Letters, Section B: Nuclear, Elementary Particle and High-Energy Physics* **721**(4-5), 252 (2013).

[3] T. Hahn, *arXiv* pp. hep–ph/0012260v2 (2000).

[4] R. Mertig, M. Bohm, A. Denner, *Computer Physics Communications* **64**(3), 345 (1991).

[5] V. Shtabovenko, R. Mertig, F. Orellana, *arXiv* p. 1601.01167 (2016).

[6] R. Mertig, R. Scharf, *Computer Physics Communications* **111**(1-3), 13 (1998).

[7] R. Sato (2013).

[8] V. Shtabovenko, *FeynHelpers : Connecting FeynCalc to FIRE and.*

[9] A. Grozin, *Arxiv preprint hepph0508242* p. 103 (2005).

[10] S. P. Martin, *arXiv* (0307101), 1 (2003).

[11] F. Staub, *Computer Physics Communications* **185**, 1773 (2014).

[12] B. Ostdiek (2), 8 (2015).

[13] D. M. Pierce (June) (1996).